

Wirtinger Flow Meets Constant Modulus Algorithm: Revisiting Signal Recovery for Grant-Free Access

Carlos Feres, *Student Member, IEEE*, Zhi Ding, *Fellow, IEEE*

Department of Electrical and Computer Engineering

University of California, Davis

Davis, CA, US

Abstract—In this work, we analyze the convergence of constant modulus algorithm (CMA) in blindly recovering multiple signals to facilitate grant-free wireless access. The CMA typically solves a non-convex problem by utilizing stochastic gradient descent. The iterative convergence of CMA can be affected by additive channel noise and finite number of samples, which is a problem not fully investigated previously. We point out the strong similarity between CMA and the Wirtinger Flow (WF) algorithm originally proposed for Phase retrieval. In light of the convergence proof of WF under limited data samples, we adopt the WF algorithm to implement CMA-based blind signal recovery. We generalize the convergence analysis of WF in the context of CMA-based blind signal recovery. Numerical simulation results also corroborate the analysis.

Index Terms—Constant-modulus algorithm, Wirtinger Flow, blind signal recovery, optimization.

I. INTRODUCTION

Recent advances in next generation networking technologies are enabling ubiquitous connection for a broad range of sensors, devices, and processors in developing smart cities, hazard monitoring, and intelligent transportation systems, among other applications [1]. Generally, wireless networks are based on either random access (e.g., WiFi) or controlled scheduling (e.g., cellular). Contention based random access schemes, such as the CSMA-CA protocol adopted in IEEE 802.11a/g/n/ac, possess the advantage of simplicity but suffer from lower spectrum efficiency due to access collision when the number of active devices is large. Controlled user scheduling based on centralized access grants can achieve high spectrum efficiency but requires elaborate network-user interaction and higher energy consumption. A typical IoT application involves sporadic communications of small amounts of data between a significant number of transceivers, triggered by external events. Such systems are better served by low-latency and grant-free communications.

In grant-free access, multiple unscheduled signal transmissions could collide at receivers [2]. A classical solution is exploit spread-spectrum for interference suppression and signal recovery by using near-orthogonal sequences such as CAZAC sequences, which exhibit high autocorrelation when synchronized, and low cross-correlations among different sequences. Unfortunately, the number of such sequences is limited. Another approach is to implement joint multi-user signal detection at the receiving access station [3], [4]. However, such receivers require rather accurate channel state information

to mitigate co-channel interference effect, thereby requiring significant pilot/training overhead for synchronization and channel estimation.

Hence, existing approaches face at least two challenges in massive IoT deployment. First, transmitting pilot or training signals consumes precious device energy and bandwidth resources in large scale IoT deployment. Such extra overhead can be significant when data packets are short as in IoT scenarios. Second, to reduce training overhead requires shorter pilot sequences. However, to accommodate grant free access for a large number of IoT devices, many orthogonal training sequences are required. Since the number of available orthogonal sequences equals to the sequence length, massive IoT deployment further exacerbate the pilot overhead problem. Clearly, for IoT applications involving large number of devices in grant-free applications, the burden on both spectrum and power [5] strongly motivates the investigation and deployment of blind signal receivers.

Thus, blind signal recovery techniques deserve a re-examination for its ability to support grant-free access and its potential to improve IoT power and bandwidth efficiency. Blind signal recovery such as blind equalization and blind source separation [6] does not require known pilots or preambles for channel probing. By exploiting high-order statistics or known characteristics of source signals, receivers can recover source signals directly from outputs of unknown linear dynamic channels.

The Constant Modulus Algorithm (CMA) by Godard [7] is perhaps the best known blind algorithm owing to its simplicity and practical effectiveness [6]. CMA has also been shown as global convergent in noiseless scenarios under full rank channel conditions [8]. CMA minimizes a non-convex cost function which traditionally uses stochastic gradient descent iteration. Other works have further proposed different variations to the basic stochastic gradient descent algorithm. However, one of its major issues in its practical applications is the presence of local minima in the constant modulus (CM) cost function as a result of additive channel noise [9], [10]. The convergence properties of such stochastic gradient descent algorithms have not been fully understood under limited samples and additive channel noise [6], [11], [12].

An alternative approach is to minimize the CM cost is to transform the CM cost minimization into a convex optimization problem via semidefinite relaxation [13]–[15]. However, the semidefinite relaxation requires lifting of parameter space to the extent that the problem size grows drastically. For multiple users and large number of parameters, such convex

This material is based upon work supported by the National Science Foundation under Grants No. 2009001, No. 1711823, and No. 1824553. C. Feres is also supported by CONICYT PFCHA/BCH 72170648 scholarship.

CMA algorithms become rather impractical in many scenarios. Furthermore, projection from high-dimensional positive semidefinite matrix back to the original parameter space via rank 1 decomposition remains difficult and elusive [16].

Another alternative line of attack tries to solve CMA problems analytically [17], [18]. These solutions and its variants [19], [20] are not iterative with direct analytical solutions. They tend to be more complex in general, and usually require stricter assumptions, such as constant modulus of the modulation symbols. There are also multistage schemes [21], that depend heavily on the estimation error being close to the MMSE estimate in the first stages; otherwise the error would accumulate substantially through different stages [22].

In recent years, there has been a strong wave of renewed interest in developing faster and more robust algorithms to directly solve the originally nonconvex optimization problems. Among a number of successful outcomes are the phase retrieval [23], [24], matrix completion [25], [26], and blind demixing of multiple sources [27], among others. Direct solutions are attractive for several reasons. First, they do not require parameter lifting into a higher dimensional space that makes larger size problems such as multiple source recovery prohibitive. Second, they do not require the additional projection back into the original parameter space and tend to provide more consistent results. Third, their performance analysis is more direct and offers better insight in terms of convergence characteristics. They do not require large problem size or approximate relaxations. Thus, these techniques can be better suited for grant-free access in resource limited networks.

In this paper, we consider a prominent non-convex algorithm known as Wirtinger Flow (WF) for minimizing the constant modulus cost. The WF algorithm has shown strong promises recently in the literature related to the blind signal recovery problem, both in terms of single source or multiple sources recovery. Our major contributions in this work are as follows. We demonstrate that the WF algorithm in the context of CMA is in fact a generalization of the phase retrieval problem that has recently gathered a lot of interest [23], [24]. In fact, we can formulate the CM minimization as Phase Retrieval based on mean amplitude information. Another interesting observation is that the WF algorithm for CM cost minimization in fact coincides with the previously proposed “normalized” CMA or NCMA. The convergence properties of NCMA have only been addressed via simulation examples. Our major contribution lies in the analysis of WF to clearly characterize the convergence conditions of WF-based CMA and identify explicit choices of the iteration stepsize.

We organize our manuscript as follows. Section II presents the signal model for blind recovery problem and the formulation for minimization of constant modulus cost. We shall discuss the basic properties of the CM cost functions. Section III introduces the proposed WF-based optimization algorithms for the single-source and multi-source recovery problem. We show that the WF algorithms in fact coincide with NCMA. Section IV provides detailed theoretical convergence properties and complexity analysis of the proposed algorithms. Section V presents numerical simulations in different scenarios, and finally Section VI concludes the work.

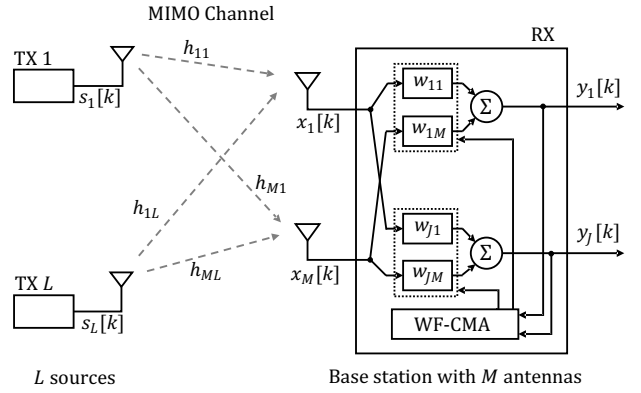


Fig. 1: System model. In every resource block, L sources share the channel and transmit independent signals to a receiver station with M antennas through an unknown physical channel. An adaptive algorithm finds J combiners to recover different sources with no interference.

Notations: In the following, vectors and matrices will be denoted with small and capital boldface letters, such as \mathbf{z} and \mathbf{Z} respectively. Complex conjugation is denoted with \bar{z} . The transpose, element-wise complex conjugation and conjugate transpose are denoted by \mathbf{z}^T , \bar{z} and \mathbf{z}^H , respectively. For a complex scalar a , we use $\text{Re}(a)$, $\text{Im}(a)$, $|a|$ and $\angle(a)$ to denote its real part, imaginary part, magnitude and angle, respectively. The Euclidean norm of vectors and spectral norm of matrices is denoted by $\|\cdot\|$. $\text{diag}(\mathbf{z})$ represents a diagonal matrix that uses elements of vector \mathbf{z} on its diagonal, and we define the operator $\text{ddiag}(\mathbf{Z})$ which yields a diagonal matrix which only retains the diagonal elements of \mathbf{Z} . $\mathbb{E}\{\cdot\}$ denotes expectation. Finally, $\mathbf{1}[\text{expr}]$ is the indicator function, that is equal to 1 if expr is true, and 0 otherwise.

II. SYSTEM MODEL

A. Blind Signal Recovery and Demixing

We consider the signal recovery of multiple users in an access group in a grant-free access system, as depicted in Fig.1. In particular, all potential uplink users in each access group have acquired timing such that their uplink signal transmission would occupy a given set of slots. The users within each access group can randomly decide to transmit within their allocated channel resources. Appropriate coding and rate-matching is utilized by all source nodes to have equal number of data symbols K within each access burst. Furthermore, we assume that with very high probability that the number of single-antenna active nodes L shall fall below the number of diversity antennas M at the receiver node. In particular, the receiver node does not necessarily know L . Since the receiver recovers multiple user signals during blind demixing without prior knowledge of their identities, the receiver can utilize user-ID scrambled CRC to check which recovered user signal belongs to which user, similar to the blind detection of PDCCH by users using RNTI-scrambled CRC in LTE [28], [29].

Thus, we define the received signal vector \mathbf{x}_k , the transmitted signal vector \mathbf{s}_k , and the flat fading channel \mathbf{H} , respectively, as

$$\mathbf{x}_k = \begin{bmatrix} x_1[k] \\ \vdots \\ x_M[k] \end{bmatrix}, \mathbf{s}_k = \begin{bmatrix} s_1[k] \\ \vdots \\ s_L[k] \end{bmatrix}, \mathbf{H} = \begin{bmatrix} h_{11} & \cdots & h_{1L} \\ \vdots & \cdots & \vdots \\ h_{M1} & \cdots & h_{ML} \end{bmatrix}. \quad (1)$$

Then the received signal vector can be written as

$$\mathbf{x}_k = \mathbf{H}\mathbf{s}_k + \mathbf{n}_k, \quad (2)$$

where the MIMO channel matrix $\mathbf{H} \in \mathbb{C}^{M \times L}$ is assumed to have full column rank (with $L \leq M$) and $\mathbf{n}_k \in \mathbb{C}^M$ is the vector of AWGN in that resource block, following the same convention as Eq.(1).

In blind demixing or blind signal recovery, we are interested in finding vectors $\mathbf{w}_j \in \mathbb{C}^M$, $j \in \{1, \dots, J\}$ that allow the recovery of J sources with minimal interference, that is,

$$y_j[k] = \mathbf{w}_j^H \mathbf{x}_k \approx \hat{s}_{\ell_j}[k], \quad \text{for source } \ell_j \in \{1, \dots, L\}, \quad (3)$$

where in particular the receiving node has no explicit knowledge on the unknown channels \mathbf{H} , except for the statistical properties and the constellation of each source signal.

First, we consider the recovery of a single source recovery. Godard in [7] proposed the well known constant modulus algorithm (CMA) to adaptively find the optimum demixer $\hat{\mathbf{w}} \in \mathbb{C}^M$ by minimizing the mean CM cost

$$E\{|y_k|^2 - R_2\}^2, \quad R_2 = \frac{E\{|s_\ell[k]|^4\}}{E\{|s_\ell[k]|^2\}}. \quad (4)$$

Despite its name, CMA can be applied to i.i.d. signals using QAM constellations of arbitrary size and magnitude [6]. Though the selection of R_2 requires the distribution information of the QAM sources, it is well known that by selecting R_2 arbitrarily, the CMA algorithm would ideally converge and recover a source signal subject to scalar ambiguity and source permutation. The output would scale the original QAM signals by a simple scalar a , without affecting signal recovery.

In batch implementation, the CM cost can be rewritten as

$$f(\mathbf{w}) = \frac{1}{2K} \sum_{k=1}^K \left(|\mathbf{x}_k^H \mathbf{w}|^2 - R_2 \right)^2, \quad (5)$$

which is a smooth real-valued nonconvex function of \mathbf{w} . Note that f presents phase invariance, i.e., if $\hat{\mathbf{w}}$ is a solution that minimizes $f(\hat{\mathbf{w}})$, then the set $\mathcal{W}(\hat{\mathbf{w}}) = \{e^{i\theta} \hat{\mathbf{w}} : \theta \in [0, 2\pi]\}$ contains equivalent solutions that achieve the minimum $f(\hat{\mathbf{w}})$.

B. Multiple Signal Recovery

In the context of massive IoT, however, multiple devices may access the channel in a grant-free scenario. To recover the multiple source signals mixed by the unknown channel \mathbf{H} , we can construct multiple demixer vectors \mathbf{w}_j , $j \in \{1, \dots, J\}$, each tuned to different signals:

$$\mathbf{y}_k = \begin{bmatrix} \mathbf{w}_1^H \\ \vdots \\ \mathbf{w}_J^H \end{bmatrix} \mathbf{x}_k = \begin{bmatrix} \hat{s}_{\ell_1}[k] \\ \vdots \\ \hat{s}_{\ell_J}[k] \end{bmatrix}, \quad \ell_j \in \{1, \dots, L\}. \quad (6)$$

Now, considering blind recovery of multiple sources, one could try to minimize the CM cost in hope of recovering one individual output each time. One could use successive interference cancellation (SIC) to remove the recovered signal contribution from the received signal \mathbf{x}_k before minimizing the CM cost again to recover another signal. SIC has a well known shortcoming of error propagation. If we attempt to simultaneously recover multiple sources by solving for multiple demixer vectors $\mathbf{w}_j \in \{1, \dots, J\}$, we need to ensure that they do not restore the same source signal, possibly with different phases or delays [6]. Therefore, when considering simultaneous multiple signal recovery, additional adjustment must be incorporated for demixers \mathbf{w}_j , $j \in \{1, \dots, J\}$ to recover different source signals. Given that the different sources are independent, this is equivalent to force statistical uncorrelatedness of the signals in the cost function. For the case of complex outputs y_{j_1}, y_{j_2} , their covariance is given by:

$$\begin{aligned} \text{Cov}\{y_{j_1}, y_{j_2}\} &= \mathbb{E}\{y_{j_1} y_{j_2}^*\} = \mathbb{E}\{\mathbf{w}_{j_1}^H \mathbf{x}_k (\mathbf{w}_{j_2}^H \mathbf{x}_k)^*\} \\ &= \mathbf{w}_{j_1}^H \mathbb{E}\{\mathbf{x}_k \mathbf{x}_k^H\} \mathbf{w}_{j_2}. \end{aligned} \quad (7)$$

Thus, we propose to use regularize the CMA cost function with the magnitude squared of the pairwise covariances of the outputs, to obtain a smooth real-valued cost function. The modified CMA cost function for multiple sources is

$$g(\mathbf{w}_1, \dots, \mathbf{w}_J) = \sum_{j=1}^J f(\mathbf{w}_j) + \gamma_0 \sum_{j_1 \neq j_2}^J |\mathbf{w}_{j_1}^H \mathbf{R}_x \mathbf{w}_{j_2}|^2, \quad (8)$$

where $\gamma_0 > 0$ is a constant and the sample covariance matrix

$$\mathbf{R}_x = \frac{1}{K} \sum_{k=1}^K \mathbf{x}_k \mathbf{x}_k^H. \quad (9)$$

This is related to the regularization proposed in [30] which uses joint cumulants for source separation. The joint cumulants also consider the potential correlatedness of delayed versions of the demixer outputs, but in the presented case of source recovery the channels have no ISI, and the information from different delays of the outputs is not necessary.

III. WF-BASED CONSTANT MODULUS SOLUTIONS

A. CMA meets Wirtinger Flow

A recent stream of nonconvex optimization procedures have been developed for solving quadratic equations, in particular for the phase retrieval problem. The phase retrieval problem can be stated as the recovery of an unknown signal \mathbf{z} using known sampling vectors \mathbf{a}_k from magnitudes $r_k = |\mathbf{a}_k^H \mathbf{z}|^2$ only for which the smooth cost function is

$$\min_{\mathbf{z} \in \mathbb{C}^M} \frac{1}{2K} \sum_{k=1}^K \left(|\mathbf{a}_k^H \mathbf{z}|^2 - r_k \right)^2. \quad (10)$$

Note that in terms of the cost functions, phase retrieval is equivalent to the CMA problem in Eq.(5), by setting $r_k = R_2$ and $\mathbf{a}_k = \mathbf{x}_k$, $k \in \{1, \dots, K\}$, and using \mathbf{z} as the unknown variable. If the source signal has constant modulus, e.g., $|s_\ell[k]|^2 = R_2$ for PSK signals, then the CM cost is the same as in the phase retrieval. On the other hand, for non-constant

modulus source signals, e.g. 16-QAM, the CM cost is akin to phase retrieval based on an ‘‘average magnitude’’.

This similarity stimulates this study on the link between optimization methods for phase retrieval and the CMA problem. However, there are some fundamental differences: (A) In phase retrieval, there is a known reference signal r_k as ground truth which is fully exploited in its convergence analysis. However, in CM-based demixing we only have a desired ‘‘average magnitude’’ R_2 . (B) Phase retrieval has only one solution (up to common rotations), where in blind demixing, there may be many ideal demixer vectors to recover multiple source signals in different order (up to common rotations). (C) The sampling vectors \mathbf{a}_k are chosen typically as Gaussian by users in phase retrieval. In CMA, \mathbf{x}_k is (noisy) channel output that is not under user control and has a more complex distribution. (D) In phase retrieval, the signal \mathbf{z} typically does not have additional constraints, whereas in CMA, the parameter vector \mathbf{w} does not have other constraints but the source signals often do.

B. Wirtinger Flow in Phase Retrieval

For such a problem formulation, the *Wirtinger Flow* (WF) presented in [23] has received considerable attention as it guarantees convergence to a solution via gradient-descent with only $\mathcal{O}(M \log M)$ measurements with Gaussian sampling vectors, obtaining ϵ -accuracy within $\mathcal{O}(KM^2 \log \epsilon)$ iterations. This algorithm has received significant research attention and several works have improved WF for the phase retrieval problem [31]–[33] or adapted WF for seemingly different and unrelated optimization problems [27], [34].

In more depth, WF is a two stage approach consisting in spectral initialization and gradient descent updates. The latter is characterized by the notion of Wirtinger calculus (also known as $\mathbb{C}\mathbb{R}$ -calculus [35]). The gradient of a real value function $p(\mathbf{z})$ with respect to a complex variable vector $\mathbf{z} = \mathbf{z}_r + i\mathbf{z}_i$ can be simply viewed as a complex vector

$$\nabla_{\mathbf{z}} p(\mathbf{z}) = \frac{\partial p(\mathbf{z})}{\partial \mathbf{z}_r} + i \frac{\partial p(\mathbf{z})}{\partial \mathbf{z}_i}. \quad (11)$$

The same principle applies when deriving Hessians.

Spectral initialization yields (with high probability) an initial iterate for gradient descent that is located within the basin of attraction of the ground truth, that is, a neighborhood of the ground truth with defined convexity and smoothness. Defining

$$\mathbf{R}_a = \frac{1}{K} \sum_{k=1}^K r_k \mathbf{a}_k \mathbf{a}_k^H, \quad (12)$$

the initial iterate is a properly scaled eigenvector of \mathbf{R}_a corresponding to its leading eigenvalue. This initial iterate is then highly correlated with ground truth, and has been proven to be close to the ground truth with high probability [23].

C. Wirtinger Flow for Single Source Recovery (SSR)

We now reformulate WF for our CM-based source recovery problem. Using $\mathbb{C}\mathbb{R}$ -calculus, the gradient of the CMA objective function f can be defined as

$$\nabla_{\mathbf{w}} f(\mathbf{w}) = \frac{1}{K} \sum_{k=1}^K \left(|\mathbf{x}_k^H \mathbf{w}|^2 - R_2 \right) \mathbf{x}_k \mathbf{x}_k^H \mathbf{w}, \quad (13)$$

and the gradient descent rule is

$$\mathbf{w}^{t+1} = \mathbf{w}^t - \frac{\mu}{K \|\mathbf{w}^t\|^2} \sum_{k=1}^K \left(|\mathbf{x}_k^H \mathbf{w}^t|^2 - R_2 \right) \mathbf{x}_k \mathbf{x}_k^H \mathbf{w}^t, \quad (14)$$

where the stepsize $\mu > 0$ could be constant or vary, either as a predefined function of the iteration t [23] or using an adaptive approach such as backtracking [36], among others.

This gradient rule, which notably shows a normalization factor, has in fact been previously introduced for the CM problem as Normalized CMA [37]–[39]. The idea is similar to normalized LMS by adjusting the stepsize in to avoid parameter divergence. Nevertheless, existing works have not thoroughly analyzed how to select the stepsize μ in NCMA, often resorting to trial-and-error. By connecting CMA to WF, we aim to define the stepsize selection according to the local geometry of CMA, thereby simplifying implementation and improving the algorithm convergence rate. We call this new approach WF-based Constant Modulus Algorithm or WF-CMA.

Applying the spectral initialization of [23] for blind source recovery yields the covariance matrix of the received signal vectors \mathbf{x}_k (corresponding to the known observations) scaled by the constant R_2 (corresponding to desired outcomes):

$$\frac{1}{K} \sum_{k=1}^K R_2 \mathbf{x}_k \mathbf{x}_k^H = R_2 \mathbf{R}_x. \quad (15)$$

The initial iterate for gradient descent is then chosen as $\mathbf{w}^0 = \eta \hat{\mathbf{v}}_1$, where $\hat{\mathbf{v}}_1$ is the normalized eigenvector corresponding to the largest eigenvalue of $R_2 \mathbf{R}_x$, and the magnitude η is equal to

$$\eta = \sqrt{\frac{M \sum_k R_2}{\sum_k \|\mathbf{x}_k\|^2}} = \sqrt{\frac{MK R_2}{\sum_k \mathbf{x}_k^H \mathbf{x}_k}}. \quad (16)$$

Algorithm 1 summarizes the steps for WF-CMA single source recovery.

Algorithm 1 WF-CMA for Single Source Recovery

Given: $\mathbf{x}_k \in \mathbb{C}^M$, $k \in \{1, \dots, K\}$, number of iterations T and stepsize μ

A) Spectral Initialization:

- 1: Compute $\eta = \sqrt{\frac{MK R_2}{\sum_k \|\mathbf{x}_k\|^2}}$
- 2: Let $\hat{\mathbf{v}}_1$ be the normalized eigenvector corresponding to the largest eigenvalue of $\frac{R_2}{K} \sum_{k=1}^K \mathbf{x}_k \mathbf{x}_k^H$
- 3: Set $\mathbf{w}^0 = \eta \hat{\mathbf{v}}_1$

B) Gradient Descent:

- 4: **for** $t = 0, \dots, T - 1$ **do**
 - 5: $\mathbf{w}^{t+1} = \mathbf{w}^t - \frac{\mu}{K \|\mathbf{w}^t\|^2} \sum_{k=1}^K \left(|\mathbf{x}_k^H \mathbf{w}^t|^2 - R_2 \right) \mathbf{x}_k \mathbf{x}_k^H \mathbf{w}^t$
 - 6: **end for**
-

D. Wirtinger Flow for Multiple Signal Recovery (MSR)

In the case of multiple signal recovery, we can apply the same principles. Using the sample covariance matrix in the

cost function of (8), gradients with respect to each demixer vector \mathbf{w}_j are

$$\begin{aligned} \nabla_{\mathbf{w}_j} g &= \frac{1}{K} \sum_{k=1}^K \left(|\mathbf{x}_k^H \mathbf{w}_j|^2 - R_2 \right) \mathbf{x}_k \mathbf{x}_k^H \mathbf{w}_j \\ &\quad + 2\gamma_0 \sum_{i \neq j}^J \mathbf{R}_x \mathbf{w}_i \mathbf{w}_i^H \mathbf{R}_x \mathbf{w}_j, \end{aligned} \quad (17)$$

and the new update rule is

$$\mathbf{w}_j^{t+1} = \mathbf{w}_j^t - \frac{\mu}{\|\mathbf{w}_j^t\|^2} \nabla_{\mathbf{w}_j} g(\mathbf{w}_1^t, \dots, \mathbf{w}_J^t). \quad (18)$$

Analogously, spectral initialization in this case is an extension of the single source case, and considers the J unit eigenvectors corresponding to the J largest eigenvalues of \mathbf{R}_x :

$$\mathbf{w}_j^0 = \sqrt{\lambda_j} \hat{\mathbf{v}}_j, \quad j \in \{1, \dots, J\}, \quad (19)$$

where λ_j is the j -th leading eigenvalue of \mathbf{R}_x and $\hat{\mathbf{v}}_j$ is its corresponding eigenvector, normalized to unit magnitude.

Algorithm 2 WF-CMA Multiple Source Recovery

Given: $\mathbf{x}_k \in \mathbb{C}^M$, $k \in \{1, \dots, K\}$, number of sources to recover J , number of iterations T and stepsize μ

A) Spectral Initialization:

- 1: Compute the J leading eigenvalues λ_j and corresponding normalized eigenvectors $\hat{\mathbf{v}}_j$ of $\frac{R_2}{K} \sum_{k=1}^K \mathbf{x}_k \mathbf{x}_k^H$
- 2: Set $\mathbf{w}_j^0 = \sqrt{\lambda_j} \hat{\mathbf{v}}_j \forall j \in \{1, \dots, J\}$

B) Gradient Descent:

- 3: **for** $t = 0, \dots, T - 1$ **do**
 - 4: **for** $j = 1, \dots, J$ **do**
 - 5: $\mathbf{w}_j^{t+1} = \mathbf{w}_j^t - \frac{\mu}{\|\mathbf{w}_j^t\|^2} \nabla_{\mathbf{w}_j} g(\mathbf{w}_1^t, \dots, \mathbf{w}_J^t)$
 - 6: **end for**
 - 7: **end for**
-

It is important to note that, depending on the data and channel, the initialization scheme for MSR might be ill-defined as the data samples might lead to a degenerate case that it is not possible to separate some sources [40]. Nevertheless, when considering the noiseless scenario (i.e., removing AWGN noise from the received signal vectors), the received signals are linear combinations of independent transmitted signals under independent Rayleigh channels. Thus, when $K \rightarrow \infty$, \mathbf{R}_x converges to the scaled expected value of $\mathbf{x} \mathbf{x}^H$ thanks to the Central Limit Theorem. This implies that, when K is large enough, the leading eigenvectors of \mathbf{R}_x will align with the leading eigenvectors of $\mathbb{E}\{\mathbf{x} \mathbf{x}^H\}$, up to a scaling factor.

IV. THEORETICAL CONVERGENCE ANALYSIS

A. Convergence Guarantee of CMA

The global convergence properties of CMA for PAM and QAM input signals in noiseless scenarios are well known [6, Chapters 4, 7]. The presented CMA-based single source recovery corresponds to a particular case of the MIMO-CMA blind equalizer, where the MIMO channel has zero ISI and only multi-user interference is to be suppressed. Thus, the mean CM cost of Eq.(4) has been shown to only possess

global minima, each of which corresponds to the successful recovery (demixing) of one source signal with a phase rotation in the noiseless case if the channel matrix \mathbf{H} has full column rank. In other words, if \mathbf{H} has full column rank, then the minimization of the mean CM cost leads to guaranteed global convergence in noiseless scenarios, regardless of initial conditions [41]. Moreover, if \mathbf{H} rank deficient a solution of the mean CM cost is close to optimal Wiener solutions [42], which further highlights the applicability of CMA-based blind signal recovery in the presence of multiple sources. The resulting combiner will exhibit some bounded interference, which is tolerable in most practical implementations. Nevertheless, we shall consider only the case when \mathbf{H} has full-column rank that guarantees global convergence for blind signal recovery.

We do not require the number of sources L to be known at any point. In the case that the receiver tries to recover more sources than the existing ones, i.e. $J \geq L$, the receiver would obtain L demixers that recover signals and $J - L$ demixers that only recover noise. In any case, the receiver can perform a rank estimation procedure if it needs to estimate L [43], [44].

When considering noisy channels, it is well known that channel noise introduces additional local minima to the mean CM cost function [6]. Thus, even carefully selected stepsize (based on trial and error) cannot guarantee convergence to global minima. Thus, new results that can reveal better convergence properties in stepsize selection are of special interest.

Given the known properties of the mean CM cost, what remains unclear is the convergence of CMA under finite data samples and additive noise. In this scenario, we aim to determine convergence properties for CM-based demixing by leveraging the convergence analysis of WF.

B. Adapting Wirtinger Flow to CMA

The convergence properties of the Wirtinger Flow phase retrieval have been proven in [23] for Eq.(10). However, the new WF-CMA exhibits two special characteristics different from the original WF in phase retrieval:

- The spectral initialization proposed for WF in phase retrieval [23] yields an eigendecomposition of the sample covariance matrix that is highly correlated with the ground truth in expectation, and the initial iterate is provably close to the ground truth to guarantee convergence. However, the same initialization in CMA-based SSR does not readily provide an initial estimate that is highly correlated with the problem solutions.
- The sampling vectors \mathbf{a}_k are assumed to either have a standard complex normal distribution, i.e. $\mathbf{a}_k \sim \mathcal{CN}(\mathbf{0}, \mathbf{I})$, or be admissible distributions for coded diffraction patterns (CDPs). However, the received signal vectors \mathbf{x}_k in CMA given by Eq.(2), are linear mixtures of independent source signals by the channel matrix \mathbf{H} , plus additive white Gaussian channel noise. They do not correspond in general with these sampling vector models, or even with those from recent work using subgaussian variables [45]. Moreover, the elements of \mathbf{x}_k are linear mixtures of independent QAM signals which are non-Gaussian, and are not mutually independent, a distinct issue that makes convergence analysis difficult.

We first examine spectral initialization. Consider the noiseless case and assume all source signals have equal symbol energy E_s without loss of generality. This assumption can be made as the different symbol energies of the sources $E_{s,\ell}$ can be included in the channel as $\mathbf{H} = \mathbf{H}'\mathbf{D}^{1/2}$, with \mathbf{H}' modeling only the channel fading across sources and receiver, and $\mathbf{D} = \text{diag}(E_{s,1}/E_s, \dots, E_{s,L}/E_s)$.

Taking expectation on the scaled sample covariance matrix in Eq.(15) for initialization:

$$\mathbb{E}\{R_2\mathbf{R}_x\} = \frac{R_2}{K} \sum_{k=1}^K \mathbf{H}\mathbb{E}\{\mathbf{s}_k\mathbf{s}_k^H\}\mathbf{H}^H = R_2E_s\mathbf{H}\mathbf{H}^H, \quad (20)$$

which depends on the channel but is not explicitly dependent on the solutions. From (3), the global CMA solutions satisfy

$$\hat{\mathbf{w}}^H \mathbf{H} \mathbf{s}_k = e^{i\varphi} s_{\ell_j}[k], \quad \ell_j \in \{1, \dots, L\}, \quad \theta \in [0, 2\pi]. \quad (21)$$

Thus, the optimal demixers are not directly extractable from the sample covariance matrix. Therefore, our work shall not analyze this initialization effect on WF-CMA. Nevertheless, we will show later in experiments that such initialization appears to benefit WF-CMA convergence. Thus, we still include this spectral initialization for CMA in Algorithm 1.

With respect to the dependent elements of \mathbf{x}_k , recall that the fading channel matrix has full column rank. Under this assumption, we can rewrite

$$y[k] = \mathbf{w}^H \mathbf{x}_k = \mathbf{w}^H \mathbf{H} \mathbf{s}_k + \mathbf{w}^H \mathbf{n}_k = \mathbf{q}^H \mathbf{s}_k + \check{n}[k], \quad (22)$$

where $\mathbf{q} = \mathbf{H}^H \mathbf{w}$ is the combined (channel plus demixer) parameter vector, and \check{n}_k is demixer output noise. Given full column rank \mathbf{H} , we can study the WF-CMA in the combined parameter space \mathbf{q} , which directly interacts with independent source signals. This parameter transformation mitigates the challenge posed by dependent signals in the WF algorithm. We now study the convergence of WF in the \mathbf{q} domain since the \mathbf{q} space can be fully spanned by adjusting \mathbf{w} .

Onwards, our approach to specifying the local convergence properties of WF is to characterize the local behavior of the CM cost function in the \mathbf{q} domain, in which we describe the gradient and Hessian of the CM-cost in the neighborhood of a ground truth. We show that the local geometry near each ground truth admits convergence to a global minimum using gradient-descent based WF algorithm.

C. Convergence of WF-CMA for single source recovery

In the following, and without loss of generality, we assume that all sources use the same square QAM constellation of size Q with equally likely symbols. These correspond to discrete finite sets, and as such, signals of each source at each time k are bounded random variables, and by definition, subgaussian random variables [46, Definition 5.7]. In other words, the signal vectors \mathbf{s}_k are supported on an exponentially large set of size Q^L , and thus are subgaussian random vectors for the purposes of concentration of measure and non-asymptotic approaches [47, Section 3.4.2]. We will use this fact to support our theoretical analysis.

We also denote the second moment, fourth moment, and kurtosis of the transmitted signals as

$$m_2 = \mathbb{E}\{|s[k]|^2\}, \quad m_4 = \mathbb{E}\{|s[k]|^4\}, \quad \kappa = m_4 - 2m_2^2 < 0. \quad (23)$$

Additionally, as QAM constellations are discrete and bounded, with probability 1 we have $\forall k \in \{1, \dots, K\}$

$$|s_\ell[k]| \leq \sqrt{\frac{3m_2}{Q-1}}(\sqrt{Q}-1) = B \Rightarrow \|\mathbf{s}_k\| \leq B\sqrt{L}. \quad (24)$$

We need some definitions. Let \mathbf{z} be a solution to the CM cost in the \mathbf{q} -domain, i.e. \mathbf{z} minimizes $f(\cdot)$. Also, note that \mathbf{z} is related only to the channel \mathbf{H} as implied in Eqs.(21) and (22), is independent of the signals \mathbf{s}_k . For any vector $\mathbf{q} \in \mathbb{C}^L$ we define

$$\text{dist}(\mathbf{q}, \mathbf{z}) = \min_{\phi \in [0, 2\pi]} \|\mathbf{q} - e^{i\phi} \mathbf{z}\|. \quad (25)$$

We define a set of solutions due to a rotation factor ϕ as

$$P := \{e^{i\phi} \mathbf{z} : \phi \in [0, 2\pi]\} \quad (26)$$

and the set of vectors within ϵ distance from P is

$$E(\epsilon) := \{\mathbf{q} \in \mathbb{C}^L : \text{dist}(\mathbf{q}, P) \leq \epsilon\}. \quad (27)$$

For any $\mathbf{q} \in \mathbb{C}^L$, we define the alignment phase $\phi(\mathbf{q})$ as

$$\phi(\mathbf{q}) := \arg \min_{\phi \in [0, 2\pi]} \|\mathbf{q} - e^{i\phi} \mathbf{z}\| = \angle(\mathbf{z}^H \mathbf{q}), \quad (28)$$

such that

$$\text{dist}(\mathbf{q}, \mathbf{z}) = \|\mathbf{q} - e^{i\phi(\mathbf{q})} \mathbf{z}\|. \quad (29)$$

By defining

$$\mathbf{A}(\mathbf{q}) = \frac{1}{K} \sum_{k=1}^K |s_k^H \mathbf{q}|^2 \mathbf{s}_k \mathbf{s}_k^H, \quad (30a)$$

$$\mathbf{B}(\mathbf{q}) = \frac{1}{K} \sum_{k=1}^K (s_k^H \mathbf{q})^2 \mathbf{s}_k \mathbf{s}_k^T, \quad \mathbf{S} = \frac{1}{K} \sum_{k=1}^K \mathbf{s}_k \mathbf{s}_k^H, \quad (30b)$$

the Wirtinger Hessian of the cost function f is simply

$$\nabla^2 f(\mathbf{q}) = \begin{bmatrix} 2\mathbf{A}(\mathbf{q}) - R_2\mathbf{S} & \mathbf{B}(\mathbf{q}) \\ \mathbf{B}(\mathbf{q}) & 2\mathbf{A}(\mathbf{q}) - R_2\mathbf{S} \end{bmatrix}. \quad (31)$$

We now present our main convergence result for single source recovery.

Theorem 1. *Consider the signal vectors $\mathbf{s}_k \in \mathbb{C}^L$ with i.i.d. elements from a square QAM constellation. Let \mathbf{z} be a solution of the CMA problem with cost function (5). Additionally, let $\alpha \geq 30$, $\beta \geq 580$, $\epsilon = (2B\sqrt{L})^{-1}$ and $\delta = 0.1$. Then, there exist $C_1 > 0$ and $c_1 > 0$ such that, if the number of measurements $K \geq C_1 L$, then for all $\mathbf{q} \in E(\epsilon)$, the cost function $f(\cdot)$ satisfies the generalized regularity condition*

$$\text{Re}\left(\langle \nabla f(\mathbf{q}), \mathbf{q} - e^{i\phi(\mathbf{q})} \mathbf{z} \rangle\right) \geq \frac{1}{\alpha} \text{dist}^2(\mathbf{q}, \mathbf{z}) + \frac{1}{\beta} \|\nabla f(\mathbf{q})\|^2 \quad (32)$$

with probability at least $1 - 6e^{-c_1 K}$. Furthermore, by selecting a stepsize $0 < \mu \leq 2/\beta$, if $\mathbf{q}^t \in E(\epsilon)$, then the update of Algorithm 1

$$\mathbf{q}^{t+1} = \mathbf{q}^t - \mu \nabla f(\mathbf{q}^t) \quad (33)$$

leads to $\mathbf{q}^{t+1} \in E(\epsilon)$ and the contraction

$$\text{dist}^2(\mathbf{q}^{t+1}, \mathbf{z}) \leq \left(1 - \frac{2\mu}{\alpha}\right) \text{dist}^2(\mathbf{q}^t, \mathbf{z}). \quad (34)$$

The proof of Theorem 1 is an extension and modification of the original Wirtinger Flow proof [23], but considering sub-gaussian signal vectors (QAM constellations) and an average modulus, as the actual magnitude samples are unknown. The steps of the proof are summarized below:

- 1) **Establishing concentration of measure of the Hessian and deriving related scalar inequalities.** In Lemma 1, we show that with high probability, the WF-CMA Hessian is close to its expectation given sufficient samples.
- 2) **Characterizing the local geometry of the CMA objective function.** We show that the cost function has strong convexity and smoothness in the ϵ -vicinity of the ground truth, which are respectively proven in Lemmas 2 and 3 based on the concentration of Hessian and the resulting inequalities. These results describe the geometry of the cost function in the neighborhood of any local minimum, which are known to correspond to global minima in noiseless CMA-based equalization.
- 3) **Proving that the WF-CMA update rule is a contraction.** In Lemma 4, we finally show that the update rule is a contraction with geometric rate within the basin of attraction $E(\epsilon)$.

We first tackle the concentration of measure of the Hessian of $f(\cdot)$ in the following lemma.

Lemma 1 (Concentration of the Hessian). *Let \mathbf{z} be a solution of (5) and independent of the signal vectors \mathbf{s}_k under the setup of Theorem 1, and $\delta > 0$. Then, there exist $C_1(\delta) > 0$ and $c_1(\delta) > 0$ such that, if $K \geq C_1(\delta)L$, then*

$$\|\nabla^2 f(\mathbf{z}) - \mathbb{E}\{\nabla^2 f(\mathbf{z})\}\| \leq \delta \quad (35)$$

holds with probability at least $1 - 6e^{-c_1(\delta)K}$.

Proof. Refer to Appendix B for details. ■

The local geometry of the cost function can be characterized using both lemmas below. Combined, they yield inequality (32). In particular, Lemma 2 describes the strong convexity of the cost function, and Lemma 3 proves the cost function is well behaved near local optimizers.

Lemma 2 (Local Curvature Condition). *Assume Lemma 1 holds, and let $\alpha \geq 30$, $\epsilon = (2B\sqrt{L})^{-1}$ and $\delta = 0.1$. Then, for all vectors $\mathbf{q} \in E(\epsilon)$, the cost function $f(\cdot)$ satisfies*

$$\begin{aligned} & \text{Re}\left(\langle \nabla f(\mathbf{q}), \mathbf{q} - e^{i\phi(\mathbf{q})}\mathbf{z} \rangle\right) \\ & \geq \left(\frac{1}{\alpha} + \frac{2m_2^2 - R_2m_2 + \delta}{4}\right) \text{dist}^2(\mathbf{q}, \mathbf{z}) \\ & \quad + \frac{1}{10K} \sum_{k=1}^K \left| \mathbf{s}_k^H(\mathbf{q} - e^{i\phi(\mathbf{q})}\mathbf{z}) \right|^4. \end{aligned} \quad (36)$$

Proof. See Appendix C. ■

Lemma 3 (Local Smoothness Condition). *Assume Lemma 1 holds, and let $\beta \geq 580$, $\epsilon = (2B\sqrt{L})^{-1}$ and $\delta = 0.1$. Then, for all vectors $\mathbf{q} \in E(\epsilon)$, the cost function (\cdot) satisfies*

$$\begin{aligned} \frac{1}{\beta} \|\nabla f(\mathbf{q})\|^2 & \leq \frac{2m_2^2 - R_2m_2 + \delta}{4} \text{dist}^2(\mathbf{q}, \mathbf{z}) \\ & \quad + \frac{1}{10K} \sum_{k=1}^K \left| \mathbf{s}_k^H(\mathbf{q} - e^{i\phi(\mathbf{q})}\mathbf{z}) \right|^4. \end{aligned} \quad (37)$$

Proof. See Appendix D. ■

Finally, based on the local behavior of the cost function, we establish the contraction of the iterative rule of Algorithm 1.

Lemma 4 (Contraction of Update Rule). *Assume that the conditions of Theorem 1 hold. Further assume that $0 < \mu \leq 2/\beta$ and that $\mathbf{q}^t \in E(\epsilon)$. Consider the following update rule*

$$\mathbf{q}^{t+1} = \mathbf{q}^t - \mu \nabla f(\mathbf{q}^t). \quad (38)$$

Then, we have that $\mathbf{q}^{t+1} \in E(\epsilon)$ and

$$\text{dist}^2(\mathbf{q}^{t+1}, \mathbf{z}) \leq \left(1 - \frac{2\mu}{\alpha}\right) \text{dist}^2(\mathbf{q}^t, \mathbf{z}). \quad (39)$$

Proof. This proof follows [23, Lemma 7.10], as our problem also has non-unique global solutions. ■

D. Convergence for Multiple Source Recovery

Recall that our cost function for MSR is a simpler version of the one in [41], which has been shown to exhibit global convergence properties under noiseless full rank channel conditions. Thus, in a way similar to the SSR case, we will describe the local geometry of the CM cost for MSR and show how the WF algorithm recovers source signals with high probability. For full column rank channel matrix, we can use the overall system parameter space as in Eq.(22) by introducing $\mathbf{q} = [\mathbf{q}_1^T \dots \mathbf{q}_J^T]^T$ as the aggregation of the J demixers:

$$y_j[k] = \mathbf{w}_j^H \mathbf{x}_k = \mathbf{q}_j^H \mathbf{s}_k + \check{\eta}_j[k]. \quad (40)$$

Thus, the cost function is

$$g(\mathbf{q}) = \sum_{j=1}^J f(\mathbf{q}_j) + \gamma_0 \sum_{j_1 \neq j_2}^J |\mathbf{q}_{j_1}^H \mathbf{S} \mathbf{q}_{j_2}|^2 \quad (41)$$

where \mathbf{S} is the sample covariance matrix defined in Eq.(30b).

For the MSR proofs, we need to generalize the previous definitions. Let $\mathbf{z} = [\mathbf{z}_1^T \dots \mathbf{z}_J^T]^T \in \mathbb{C}^{JL}$ be a solution that minimizes $g(\cdot)$ and is independent of the signals \mathbf{s}_k . For any vector $\mathbf{q} \in \mathbb{C}^{JL}$,

$$\text{dist}(\mathbf{q}, \mathbf{z}) = \left(\sum_{j=1}^J \min_{\phi \in [0, 2\pi]} \|\mathbf{q}_j - e^{i\phi} \mathbf{z}_j\|^2 \right)^{\frac{1}{2}}. \quad (42)$$

We define the set of all vectors that differ from the solution by a rotation factor in each demixer as

$$P := \{[e^{i\phi_1} \mathbf{z}_1^T \dots e^{i\phi_J} \mathbf{z}_J^T]^T : \phi_j \in [0, 2\pi] \quad \forall j \in \{1, \dots, J\}\}. \quad (43)$$

The sets of vectors close to P and P_i are

$$E(\epsilon) := \{\mathbf{q} \in \mathbb{C}^{JL} : \text{dist}(\mathbf{q}, P) \leq \epsilon\}, \quad (44)$$

and, for any vector $\mathbf{q} \in \mathbb{C}^{JL}$ we define the phases $\phi_i(\mathbf{q})$ as

$$\phi_j(\mathbf{q}) := \phi(\mathbf{q}_j) = \arg \min_{\phi \in [0, 2\pi]} \|\mathbf{q}_j - e^{i\phi} \mathbf{z}_j\| = \angle(\mathbf{z}_j^H \mathbf{q}_j) \quad (45)$$

such that

$$\text{dist}(\mathbf{q}, \mathbf{z}) = \left(\sum_{j=1}^J \|\mathbf{q}_j - e^{i\phi(\mathbf{q}_j)} \mathbf{z}_j\|^2 \right)^{\frac{1}{2}}. \quad (46)$$

The Wirtinger Hessian of the cost function g is

$$\begin{aligned} \nabla^2 g(\mathbf{q}) = & \text{Bdiag} \left(\left\{ \nabla^2 f(\mathbf{q}_j) \right\}_{j=1}^J \right) \\ & + 2\gamma_0 \begin{bmatrix} \mathbf{G}_1(\mathbf{q}) & \cdots & \mathbf{H}_{1,J}(\mathbf{q}) \\ \vdots & \ddots & \vdots \\ \mathbf{H}_{J,1}(\mathbf{q}) & \cdots & \mathbf{G}_J(\mathbf{q}) \end{bmatrix} \end{aligned} \quad (47)$$

where $\text{Bdiag}(\cdot)$ constructs a block diagonal matrix out of the matrices

$$\nabla^2 f(\mathbf{q}_j) = \begin{bmatrix} 2\mathbf{A}(\mathbf{q}_j) - R_2 \mathbf{S} & \mathbf{B}(\mathbf{q}_j) \\ \mathbf{B}(\mathbf{q}_j) & 2\mathbf{A}(\mathbf{q}_j) - R_2 \bar{\mathbf{S}} \end{bmatrix}. \quad (48)$$

$\mathbf{A}(\mathbf{q}_j)$, $\mathbf{B}(\mathbf{q}_j)$, and \mathbf{S} have been defined in Eq.(30) and

$$\mathbf{G}_j(\mathbf{q}) = \begin{bmatrix} \mathbf{C}_j(\mathbf{q}) & \mathbf{0} \\ \mathbf{0} & \bar{\mathbf{C}}_j(\mathbf{q}) \end{bmatrix}, \quad \mathbf{C}_j(\mathbf{q}) = \sum_{i \neq j}^J \mathbf{S} \mathbf{q}_i \mathbf{q}_i^H \mathbf{S}. \quad (49)$$

Furthermore, we have

$$\begin{aligned} \mathbf{H}_{ji}(\mathbf{q}) &= \begin{bmatrix} \mathbf{E}_{ji}(\mathbf{q}) & \mathbf{F}_{ji}(\mathbf{q}) \\ \mathbf{F}_{ji}(\mathbf{q}) & \mathbf{E}_{ji}(\mathbf{q}) \end{bmatrix}, \\ \mathbf{E}_{ji}(\mathbf{q}) &= \mathbf{q}_i^H \mathbf{S} \mathbf{q}_j \mathbf{S}, \quad \mathbf{F}_{ji}(\mathbf{q}) = \mathbf{S} \mathbf{q}_i \mathbf{q}_j^T \mathbf{S}^T. \end{aligned} \quad (50)$$

We now introduce the convergence analysis of Algorithm 2.

Theorem 2. Consider signal vectors $\mathbf{s}_k \in \mathbb{C}^L$ with elements that are i.i.d. from a square QAM constellation. Let \mathbf{z} be a solution of the MSR CMA problem with cost function (8). Moreover, let $\alpha \geq 30$, $\beta \geq 580$, $\epsilon = \sqrt{J}(2B\sqrt{L})^{-1}$, $\gamma_0 = 1$ and $\delta = 0.1$. Then, there exist $C_2 > 0$ and $c_2 > 0$ such that, if the number of samples $K \geq C_2 L$, then for all $\mathbf{q} \in E(\epsilon)$, the cost function $g(\cdot)$ satisfies the generalized regularity condition

$$\begin{aligned} \text{Re} \left(\langle \nabla_j g(\mathbf{q}), \mathbf{q}_j - e^{i\phi(\mathbf{q}_j)} \mathbf{z}_j \rangle \right) &\geq \\ &\frac{1}{\alpha} \text{dist}^2(\mathbf{q}_j, \mathbf{z}_j) + \frac{1}{\beta} \|\nabla_j g(\mathbf{q})\|^2 \end{aligned} \quad (51)$$

with probability at least $1 - 12e^{-c_2 K}$. Furthermore, by selecting a stepsize $0 < \mu \leq 2/\beta$ and $\mathbf{q}^t \in E(\epsilon)$, then the MSR WF-CMA updates from Algorithm 2

$$\mathbf{q}_j^{t+1} = \mathbf{q}_j^t - \mu \nabla_j g(\mathbf{q}^t) \quad (52)$$

will lead to $\mathbf{q}^{t+1} \in E(\epsilon)$ and

$$\text{dist}^2(\mathbf{q}^{t+1}, \mathbf{z}) \leq \left(1 - \frac{2\mu}{\alpha} \right) \text{dist}^2(\mathbf{q}^t, \mathbf{z}). \quad (53)$$

The proof of Theorem 2 follows a similar approach as proof of Theorem 1, with requisite modifications to account for the additional terms in the cost function $g(\cdot)$, i.e. the multiple CM costs for each demixer and the pairwise covariances of demixers in Eq.(41). To summarize:

- 1) **Establish concentration of measure for the MSR Hessian.** Lemma 5 proves that the MSR Hessian is also close to its expected value with high probability.
- 2) **Describe local geometry of the MSR cost function.** We show that the MSR cost function exhibits strong convexity and smoothness in the ϵ -vicinity of the ground truth. These properties are proven in Lemmas 6 and 7 by way of Lemmas 1, 2, 3 and 5.
- 3) **Prove that the MSR update is a contraction.** This is shown in Lemma 8 for iteration within the basin of attraction $E(\epsilon)$.

The detailed proofs of the following lemmas are omitted for brevity, and can be found in our supplemental material.

Lemma 5 (Concentration of the MSR Hessian). Let \mathbf{z} be a solution of (8) independent of the signal vectors \mathbf{s}_k , under the setup of Theorem 2. Then, there exists $C_2, c_2 > 0$ such that, if $K \geq C_2 L$, then

$$\|\nabla^2 g(\mathbf{z}) - \mathbb{E}\{\nabla^2 g(\mathbf{z})\}\| \leq \delta \quad (54)$$

holds with probability at least $1 - 12e^{-c_2 K}$.

Lemma 6 (MSR Local Curvature Condition). Assume Lemma 5 holds, and let $\alpha \geq 30$, $\epsilon = \sqrt{J}(2B\sqrt{L})^{-1}$, $\gamma_0 = 1$ and $\delta = 0.1$. Then, for all vectors $\mathbf{q} \in E(\epsilon)$ and all $j \in \{1, \dots, J\}$, the cost function $g(\cdot)$ satisfies

$$\begin{aligned} \text{Re} \left(\langle \nabla_j g(\mathbf{q}), \mathbf{q}_j - e^{i\phi(\mathbf{q}_j)} \mathbf{z}_j \rangle \right) &\geq \\ &\frac{1}{\alpha} \text{dist}^2(\mathbf{q}_j, \mathbf{z}_j) + \frac{2m_2^2 - R_2 m_2 + \delta}{4} \text{dist}^2(\mathbf{q}, \mathbf{z}) \\ &+ \frac{1}{10K} \sum_{k=1}^K \sum_{j=1}^J \left| \mathbf{s}_k^H(\mathbf{q}_j - e^{i\phi(\mathbf{q}_j)} \mathbf{z}_j) \right|^4. \end{aligned} \quad (55)$$

Lemma 7 (MSR Local Smoothness Condition). Assume Lemma 5 holds, and let $\beta \geq 580$, $\epsilon = \sqrt{J}(2B\sqrt{L})^{-1}$, $\gamma_0 = 1$ and $\delta = 0.1$. Then, for all vectors $\mathbf{q} \in E(\epsilon)$ and all $j \in \{1, \dots, J\}$, the cost function $g(\cdot)$ satisfies

$$\begin{aligned} \frac{1}{\beta} \|\nabla_j g(\mathbf{q})\|^2 &\leq \frac{2m_2^2 - R_2 m_2 + \delta}{4} \text{dist}^2(\mathbf{q}, \mathbf{z}) \\ &+ \frac{1}{10K} \sum_{k=1}^K \sum_{j=1}^J \left| \mathbf{s}_k^H(\mathbf{q}_j - e^{i\phi(\mathbf{q}_j)} \mathbf{z}_j) \right|^4. \end{aligned} \quad (56)$$

Lemma 8 (Contraction of MSR Update Rule). Assume all conditions in Theorem 2, and consider $\mathbf{q}^t \in E(\epsilon)$ and $0 < \mu \leq 2/\beta$. Using the update rules of Algorithm 2,

$$\mathbf{q}_j^{t+1} = \mathbf{q}_j^t - \mu \nabla_j g(\mathbf{q}^t), \quad (57)$$

we have that $\mathbf{q}^{t+1} \in E(\epsilon)$ and

$$\text{dist}^2(\mathbf{q}^{t+1}, \mathbf{z}) \leq \left(1 - \frac{2\mu}{\alpha} \right) \text{dist}^2(\mathbf{q}^t, \mathbf{z}). \quad (58)$$

E. Computational Complexity

The complexity of our algorithm lies in its initialization, its iteration, and number of iterations.

- 1) The initialization step is dominated by the computation of the sample covariance matrix \mathbf{R}_x , whose complexity

TABLE I: Computational complexity of proposed algorithms.

	Iteration (outer)	Total cost
WF-SSR	$\mathcal{O}(M^2K)$	$\mathcal{O}(M^2KT)$
WF-MSR	$\mathcal{O}(JM^2K)$	$\mathcal{O}(JM^2KT)$

is of $\mathcal{O}(M^2K)$. Computing the largest eigenvector of \mathbf{R}_x typically has a cost of $\mathcal{O}(M^2)$ [23].

- 2) The iteration cost is dominated by matrix-to-vector multiplications $\mathbf{x}_k \mathbf{x}_k^H \mathbf{w}$, whose complexity is of $\mathcal{O}(M^2K)$. Other operations including scalar multiplications and divisions are of $\mathcal{O}(M)$ or $\mathcal{O}(MK)$ for operations over sample-related quantities. Therefore, the iteration cost becomes dominant over the initialization cost after a few iterations.

The same analysis applies to multiple signal recovery with J sources. Succinctly, each operation repeats J times, as now there are J gradients. Therefore, the dominant cost of the multiple signal recovery variations for both algorithms are increased by a factor of J , and the resulting total cost is J times than the single source recovery case. Table I summarizes the complexity of both proposed algorithms, where T is the number of iterations in each case.

V. SIMULATION RESULTS

In our simulation tests, we consider a grant-free access scenario as described in Eqs.(1) and (2), in which there are L sources each sequentially transmitting K independent QAM symbols with normalized average energy. The receiver has M antennas and aims to recover J distinct sources. A stationary Rayleigh channel \mathbf{H} has i.i.d. elements $H_{ml} \sim \mathcal{N}(0, 0.5) + i\mathcal{N}(0, 0.5)$. The channel noise vector \mathbf{n}_k has i.i.d. and circularly symmetric complex normal elements $n_m[k] \sim \mathcal{CN}(0, \sigma_w^2)$. To evaluate the recovery efficacy, we measure the total interference to signal (power) ratio TISR for each recovered source [6], defined as

$$\text{TISR}_j = \frac{\sum_i |q_{j,i}|^2 - \max_i |q_{j,i}|^2}{\max_i |q_{j,i}|^2}, \quad (59)$$

where $\mathbf{q}_j = \mathbf{H}^H \mathbf{w}_j$ is the equalized channel at demixer j . In SSR tests, $J = 1$ and we can drop the j index.

Our simulation uses MATLAB on a PC with an Intel Core i7-7700HQ CPU, 16GB of RAM and 64-bit OS to implement the algorithms and run the simulations. We use $T = 1000$ iterations per run of the WF algorithm, and average 100 runs to obtain our results.

A. Single source recovery

To test the convergence of WF-CMA in SSR, we first consider an adaptive demixer to recover one source. We define a step-size $\mu = 5 \cdot 10^{-4} < 2/\beta$ as determined according to Theorem 1.

Fig. 2a presents the probability of successful recovery of a single source in a noiseless system with $L = 4$ sources and $M = 8$ receiving antennas. We define ‘‘success’’ as the event of TISR reaching below -20 dB after $T = 1000$ iterations. Two modulations (QPSK and 16-QAM) are tested. The results show that for QPSK, WF-CMA can actually converge to a

solution even with a very small number of samples. For the higher-order modulation of 16-QAM, successful convergence requires about 10 times more data samples. More important, our test results show that spectral initialization of WF achieves better convergence than the traditional initialization that sets a random, unique tap of the demixer to 1 and others as 0. The higher probability of success achieved by spectral initialization empirically justifies its additional computational cost.

Fig. 2b illustrates the average TISR under QPSK modulation under different SNR values. In this test, we used $K = 400$ samples, $L = 4$ sources and $M = 8$ receiver antennas. The results demonstrate desirable convergence with increasing number of iterations. On the other hand, Fig. 2c shows the average TISR for 16-QAM modulation under the same test settings. For QPSK, the total interference to signal ratio can drop below -27 dB even for 10 dB of SNR. For 16-QAM, the interference power remains several dB higher. Such results are expected for a more complex modulation without constant modulus. Nevertheless, as shown in our analytical results, the WF-CMA converges with the stepsize chosen according to Theorem 1 and successfully suppresses multi-user interference.

We repeat the experiments for a larger problem size of $L = 9$ sources and $M = 16$ receiver antennas. Under similar conditions, the success probability of the WF-CMA under different sample sizes K are also clearly shown in Fig. 2d. These results further demonstrate the superior performance achieved using spectral initialization. Correspondingly, the average TISR is shown in Fig. 2e and Fig. 2f for QPSK and 16-QAM, respectively. According to our analysis, we lowered the stepsize to $\mu = 10^{-4}$ since the basin of attraction for size ϵ (depending on B) decreases with the number of sources L . The resulting WF-CMA also shows successful recovery of a single source with sufficiently high interference suppression in for both QPSK and 16-QAM at different levels of SNR.

B. Multiple source recovery

We now replicate the experiments above, attempting to simultaneously recover $J = 2$ sources at a time. We also set $\gamma_0 = 1$ and $\mu = 1 \cdot 10^{-3} < 2/\beta$ according to Theorem 2.

Fig. 3a shows the probability of successful recovery of both sources given different numbers of samples in a noiseless system. We considered $L = 4$ sources, $M = 8$ receiving antennas for two different modulations of QPSK and 16-QAM. In the MSR case, success is defined as achieving less than -20 dB TISR after $T = 1000$ iterations in each demixer, both recovering distinct sources. Once again, the required number of samples for successful QPSK recovery appears quite small, whereas the number of samples required for successful 16-QAM recovery is approximately 10 times higher.

In Fig. 3b we show the average TISR of both demixers for QPSK signals under different levels of SNR. We let $K = 400$ samples, $L = 4$ sources and $M = 8$ receiver antennas. Fig. 3c shows the achieved TISR for 16-QAM signals under the same setup. For QPSK source signals, the average TISR drops below -30 dB for SNR of 20dB and 30dB within 400 iterations. For 16-QAM source signals, the convergence rate is noticeably slower as 16-QAM constellation exhibits variable moduli.

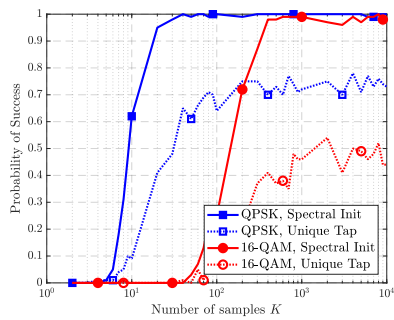
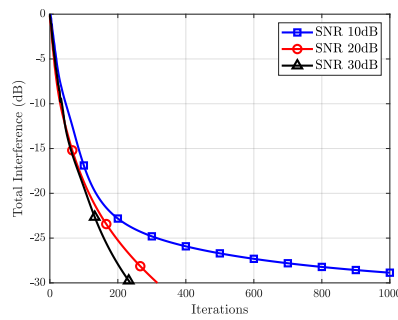
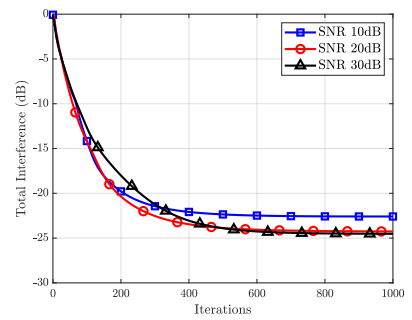
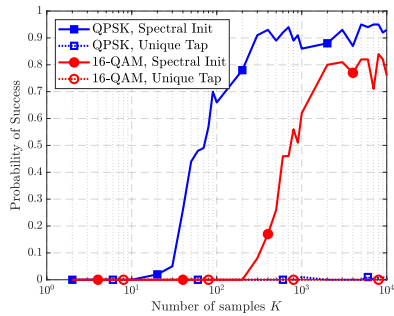
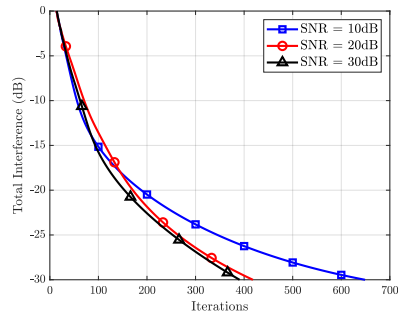
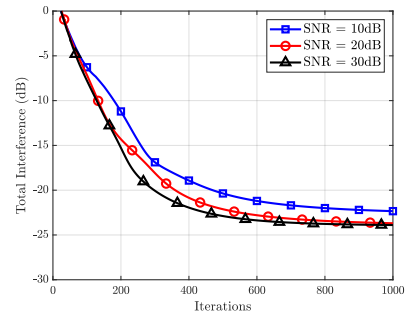
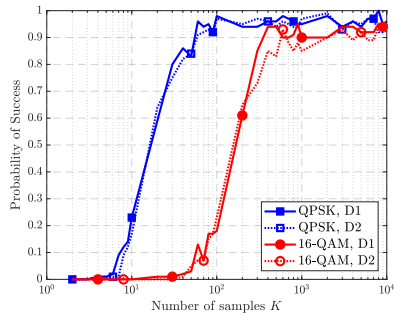
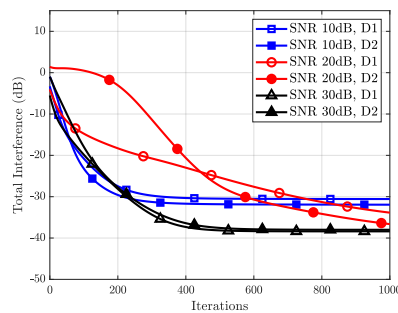
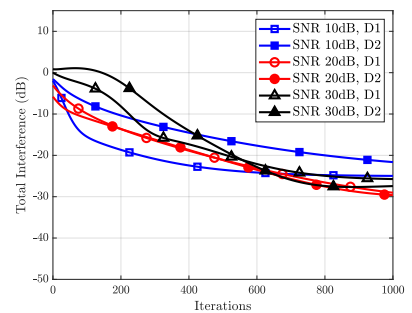
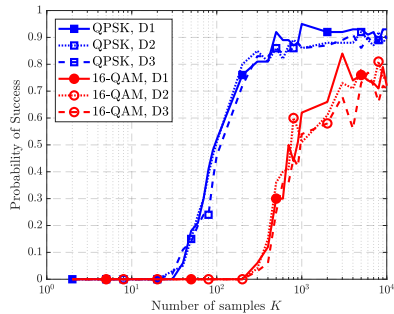
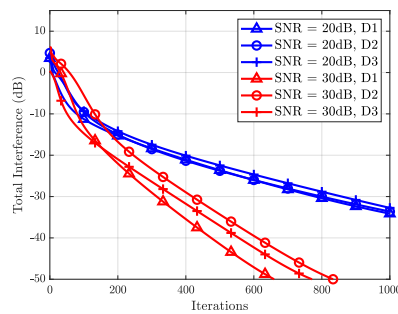
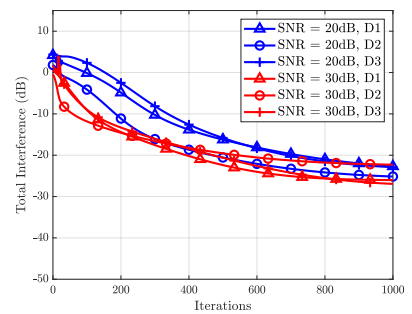
(a) Success probability, $M = 8$, $L = 4$.(b) QPSK, $M = 8$, $L = 4$.(c) 16-QAM, $M = 8$, $L = 4$.(d) Success probability, $M = 16$, $L = 9$.(e) QPSK, $M = 16$, $L = 9$.(f) 16-QAM, $M = 16$, $L = 9$.

Fig. 2: Numerical results of WF-CMA for single source recovery.

(a) Success probability, $M = 8$, $L = 4$.(b) QPSK, $M = 4$, $L = 8$.(c) 16-QAM, $M = 8$, $L = 4$.(d) Success probability, $M = 16$, $L = 9$.(e) QPSK, $M = 16$, $L = 9$.(f) 16-QAM, $M = 16$, $L = 9$.Fig. 3: Numerical results of WF-CMA for multiple source recovery. We recover either $J = 2$ or $J = 3$ signals in each setting.

Next, we also consider the larger problem size with $L = 9$ sources and $M = 16$ receiver antennas. We use a stepsize of $\mu = 10^{-4}$ for the same reasons explained in the single source recovery case. Fig. 3d shows the probability of successful recovery of both sources with under -20 dB TISR after 1000 iterations. The number of samples required for recovery increases with a larger system size, but not significantly. Fig. 3e and Fig. 3f show the achieved average TISR for QPSK and 16-QAM sources, respectively. Both figures show that WF-CMA is able to recover two signals reliably at the same time.

VI. CONCLUSION

In this work, we establish the connection between Wirtinger Flow used in phase retrieval and the constant modulus algorithm for blind signal recovery in grant-free access. As a result, we present a Wirtinger Flow algorithm for CMA-based signal recovery. We generalize the convergence analysis of WF for our WF-CMA algorithm by incorporating new conditions of subgaussian signal sources and average modulus, demonstrating its global convergence for blind signal recovery with high probability under limited data samples. We characterize the local geometry of the CM cost function in terms of smoothness and convexity, which enables parameter updates to remain within the basin of attraction for a defined stepsize. Our analysis demonstrates that the WF-CMA algorithm can solve CMA-based blind signal recovery with a fast convergence rate and reasonable computational cost.

Future work may consider stronger initialization methods with provable convergence improvement for source signals without constant modulus, or theoretical analysis and convergence properties under noisy scenarios. Other lines of research could focus on the inclusion of additional information for successful signal recovery, such as forward error correction codes, or adapting the algorithm for signals that change constellation size over the duration of the data packet, e.g. WiFi, which has QPSK preambles and M -QAM payloads.

REFERENCES

- [1] A. Al-Fuqaha, M. Guizani, M. Mohammadi, M. Aledhari, and M. Ayyash, "Internet of Things: A Survey on Enabling Technologies, Protocols, and Applications," *IEEE Communications Surveys Tutorials*, vol. 17, no. 4, pp. 2347–2376, 4th Quarter 2015.
- [2] A. Azari, P. Popovski, G. Miao, and C. Stefanovic, "Grant-Free Radio Access for Short-Packet Communications over 5G Networks," in *Proc. IEEE Global Communications Conference*, Dec 2017, pp. 1–7.
- [3] D. Ciunzo, P. S. Rossi, and S. Dey, "Massive MIMO Channel-Aware Decision Fusion," *IEEE Transactions on Signal Processing*, vol. 63, no. 3, pp. 604–619, 2015.
- [4] A. Shirazinia, S. Dey, D. Ciunzo, and P. Salvo Rossi, "Massive MIMO for Decentralized Estimation of a Correlated Source," *IEEE Transactions on Signal Processing*, vol. 64, no. 10, pp. 2499–2512, May 2016.
- [5] M. Masoudi, A. Azari, E. A. Yavuz, and C. Cavdar, "Grant-Free Radio Access IoT Networks: Scalability Analysis in Coexistence Scenarios," in *Proc. IEEE Int. Conf. on Communications*, May 2018, pp. 1–7.
- [6] Z. Ding and Y. G. Li, *Blind Equalization and Identification*. Marcel Dekker, Inc., December 2000.
- [7] D. Godard, "Self-Recovering Equalization and Carrier Tracking in Two-Dimensional Data Communication Systems," *IEEE Transactions on Communications*, vol. 28, no. 11, pp. 1867–1875, November 1980.
- [8] Ye Li and Zhi Ding, "Global Convergence of Fractionally Spaced Godard Equalizers," in *Proceedings of 1994 28th Asilomar Conference on Signals, Systems and Computers*, vol. 1, Oct 1994, pp. 617–621 vol.1.
- [9] I. Fijalkow, C. Manlove, and C. Johnson, "Adaptive fractionally spaced blind cma equalization: Excess mse," *IEEE Transactions on Signal Processing*, vol. 46, no. 1, pp. 227–231, 1998.
- [10] W. Chung and J. P. LeBlanc, "The local minima of fractionally-spaced CMA blind equalizer cost function in the presence of channel noise," in *Proc. IEEE Int. Conf. on Acoustics, Speech and Signal Processing*, vol. 6. IEEE, 1998, pp. 3345–3348.
- [11] H. H. Zeng, L. Tong, and C. R. Johnson, "An Analysis of Constant Modulus Receivers," *IEEE Transactions on Signal Processing*, vol. 47, no. 11, pp. 2990–2999, Nov 1999.
- [12] O. Dabeer and E. Masry, "Convergence Analysis of the Constant Modulus Algorithm," *IEEE Transactions on Information Theory*, vol. 49, no. 6, pp. 1447–1464, June 2003.
- [13] B. Mariere, Z.-Q. T. Luo, and T. N. Davidson, "Blind Constant Modulus Equalization via Convex Optimization," *IEEE Trans. Signal Processing*, vol. 51, pp. 805–818, 2003.
- [14] Z. Luo, W. Ma, A. M. So, Y. Ye, and S. Zhang, "Semidefinite Relaxation of Quadratic Optimization Problems," *IEEE Signal Processing Magazine*, vol. 27, no. 3, pp. 20–34, May 2010.
- [15] K. Wang, "Semidefinite Relaxation Based Blind Equalization using Constant Modulus Criterion," *CoRR*, vol. abs/1808.07232, 2018. [Online]. Available: <http://arxiv.org/abs/1808.07232>
- [16] A. Adler and M. Wax, "Constant Modulus Algorithms via Low-Rank Approximation," *Signal Processing*, vol. 160, pp. 263 – 270, 2019. [Online]. Available: <http://www.sciencedirect.com/science/article/pii/S0165168419300568>
- [17] B. Hassibi, A. Paulraj, and T. Kailath, "On a Closed Form Solution to the Constant Modulus Factorization Problem," in *Proc. 28th Asilomar Conf. on Signals, Systems and Computers*, vol. 2, Oct 1994, pp. 775–779.
- [18] A.-J. van der Veen and A. Paulraj, "An Analytical Constant Modulus Algorithm," *IEEE Trans. on Signal Processing*, vol. 44, no. 5, pp. 1136–1155, May 1996.
- [19] A.-J. van der Veen, "An Adaptive Version of the Algebraic Constant Modulus Algorithm [Blind Source Separation Applications]," in *Proc. IEEE Intl. Conf. on Acoustics, Speech, and Signal Processing*, vol. 4, March 2005, pp. iv/873–iv/876 Vol. 4.
- [20] V. Zarzoso and P. Comon, "Optimal Step-Size Constant Modulus Algorithm," *IEEE Trans. Communications*, vol. 56, no. 1, pp. 10–13, Jan. 2008.
- [21] J. J. Shynk and R. P. Gooch, "Performance Analysis of the Multistage CMA Adaptive Beamformer," in *Proceedings of MILCOM '94*, Oct 1994, pp. 316–320 vol.2.
- [22] D. Liu and L. Tong, "An Analysis of Constant Modulus Algorithm for Array Signal Processing," *Signal Processing*, vol. 73, no. 1, pp. 81 – 104, 1999. [Online]. Available: <http://www.sciencedirect.com/science/article/pii/S0165168498001868>
- [23] E. J. Candès, X. Li, and M. Soltanolkotabi, "Phase Retrieval via Wirtinger Flow: Theory and Algorithms," *IEEE Transactions on Information Theory*, vol. 61, no. 4, pp. 1985–2007, April 2015.
- [24] —, "Phase Retrieval from Masked Fourier Transforms," *CoRR*, vol. abs/1310.3240, 2013. [Online]. Available: <http://arxiv.org/abs/1310.3240>
- [25] R. H. Keshavan, A. Montanari, and S. Oh, "Matrix Completion from a Few Entries," *IEEE Trans. Inf. Theor.*, vol. 56, no. 6, pp. 2980–2998, Jun. 2010. [Online]. Available: <http://dx.doi.org/10.1109/TIT.2010.2046205>
- [26] K. Yang, Y. Shi, and Z. Ding, "Low-Rank Matrix Completion for Mobile Edge Caching in Fog-RAN via Riemannian Optimization," in *2016 IEEE Global Communications Conference*, Dec 2016, pp. 1–6.
- [27] J. Dong and Y. Shi, "Nonconvex Demixing From Bilinear Measurements," *IEEE Trans on Signal Processing*, vol. 66, no. 19, pp. 5152–5166, Oct 2018.
- [28] *Evolved Universal Terrestrial Radio Access (E-UTRA): Multiplexing and channel coding*, 3GPP Tech. Specification TS 36.212 (v13.2.0), 2016.
- [29] A. Jalali and Z. Ding, "Joint Detection and Decoding of Polar Coded 5G Control Channels," *IEEE Transactions on Wireless Communications*, vol. 19, no. 3, pp. 2066–2078, 2020.
- [30] Y. Chen, C. Nikias, and J. G. Proakis, "CRIMNO: Criterion with Memory Nonlinearity for Blind Equalization," in *Proc. 25th Asilomar Conf. on Signals, Systems Computers*, Nov 1991, pp. 694–698.
- [31] Y. Chen and E. Candes, "Solving Random Quadratic Systems of Equations Is Nearly as Easy as Solving Linear Systems," in *Advances in Neural Information Processing Systems 28*, C. C. et al., Ed. Curran Associates, Inc., 2015, pp. 739–747.
- [32] H. Zhang, Y. Liang, and Y. Chi, "A Nonconvex Approach for Phase Retrieval: Reshaped Wirtinger Flow and Incremental Algorithms," *Journal of Machine Learning Research*, vol. 18, no. 141, pp. 1–35, 2017. [Online]. Available: <http://jmlr.org/papers/v18/16-572.html>

- [33] E. Bostan, M. Soltanolkotabi, D. Ren, and L. Waller, "Accelerated Wirtinger Flow for Multiplexed Fourier Ptychographic Microscopy," *Proc. 25th IEEE Int. Conf. on Image Processing*, pp. 3823–3827, 2018.
- [34] J. Dong, Y. Shi, and Z. Ding, "Blind Over-the-Air Computation and Data Fusion via Provable Wirtinger Flow," *CoRR*, vol. abs/1811.04644, 2018. [Online]. Available: <http://arxiv.org/abs/1811.04644>
- [35] K. Kreutz-Delgado, "The Complex Gradient Operator and the CR-Calculus," *CoRR*, vol. abs/1808.07232, 2009. [Online]. Available: <http://arxiv.org/abs/0906.4835>
- [36] L. Armijo, "Minimization of functions having lipschitz continuous first partial derivatives," *Pacific J. Math.*, vol. 16, no. 1, pp. 1–3, 1966. [Online]. Available: <https://projecteuclid.org:443/euclid.pjm/1102995080>
- [37] D. L. Jones, "A Normalized Constant-Modulus Algorithm," in *Conference Record of The Twenty-Ninth Asilomar Conference on Signals, Systems and Computers*, vol. 1, Oct 1995, pp. 694–697 vol.1.
- [38] O. Tanrikulu, A. G. Constantinides, and J. A. Chambers, "New Normalized Constant Modulus Algorithms with Relaxation," *IEEE Signal Processing Letters*, vol. 4, no. 9, pp. 256–258, Sep. 1997.
- [39] K. Dogancay and O. Tanrikulu, "Normalised Constant Modulus Algorithm with Selective Partial Updates," in *2001 IEEE International Conference on Acoustics, Speech, and Signal Processing. Proceedings (Cat. No.01CH37221)*, vol. 4, May 2001, pp. 2181–2184 vol.4.
- [40] Y. M. Lu and G. Li, "Spectral Initialization for Nonconvex Estimation: High-Dimensional Limit and Phase Transitions," in *Proc. IEEE Int. Symp. on Information Theory*, June 2017, pp. 3015–3019.
- [41] Ye Li and K. J. R. Liu, "Adaptive Blind Source Separation and Equalization for Multiple-Input/Multiple-Output Systems," *IEEE Transactions on Information Theory*, vol. 44, no. 7, pp. 2864–2876, Nov 1998.
- [42] H. H. Zeng, L. Tong, and C. R. Johnson, "An analysis of constant modulus receivers," *IEEE Transactions on Signal Processing*, vol. 47, no. 11, pp. 2990–2999, 1999.
- [43] H. Akaike, "A New Look at the Statistical Model Identification," *IEEE Transactions on Automatic Control*, vol. 19, no. 6, pp. 716–723, 1974.
- [44] M. Wax and T. Kailath, "Detection of Signals by Information Theoretic Criteria," *IEEE Transactions on Acoustics, Speech, and Signal Processing*, vol. 33, no. 2, pp. 387–392, 1985.
- [45] B. Gao, H. Liu, and Y. Wang, "Phase retrieval for sub-Gaussian measurements," *CoRR*, vol. abs/1911.08710, 2019. [Online]. Available: <http://arxiv.org/abs/1911.08710>
- [46] R. Vershynin, "Introduction to the Non-Asymptotic Analysis of Random Matrices," in *Compressed Sensing: Theory and Applications*, Y. C. Eldar and G. Kutyniok, Eds. Cambridge University Press, 2012, ch. 5, pp. 210–268.
- [47] —, *High-Dimensional Probability: An Introduction with Applications in Data Science*, September 2018.

APPENDIX A: TECHNICAL LEMMAS AND COROLLARIES

Here, we establish a lemma to prove Lemma 1.

Lemma 9 (Concentration of sample covariance). *Consider independent subgaussian vectors $\mathbf{a}_k \in \mathbb{C}^L$. For every $\delta > 0$, there exist $C(\delta), c(\delta) > 0$ such that for $K \geq C(\delta)L$,*

$$\left\| \frac{1}{K} \sum_{k=1}^K \mathbf{a}_k \mathbf{a}_k^H - \mathbb{E}\{\mathbf{a}_k \mathbf{a}_k^H\} \right\| \leq \delta,$$

holds with probability at least $1 - 2e^{-c(\delta)K}$.

Proof. Subgaussian vectors \mathbf{a}_k can be defined as the independent rows of a $K \times L$ matrix A . Hence, Lemma 9 is a consequence of [46, Theorem 5.39]. ■

Corollary 10. *In the setting of Lemma 9, for $K \geq C(\delta)L$ and $\mathbf{h} \in \mathbb{C}^L$, with probability at least $1 - 2e^{-c(\delta)K}$,*

$$-\delta \|\mathbf{h}\|^2 \leq \frac{1}{K} \sum_{k=1}^K |\mathbf{a}_k^H \mathbf{h}|^2 - \mathbf{h}^H \mathbb{E}\{\mathbf{a}_k \mathbf{a}_k^H\} \mathbf{h} \leq \delta \|\mathbf{h}\|^2.$$

The expectation of matrices $A(\mathbf{q})$ and $B(\mathbf{q})$ are:

$$\begin{aligned} \mathbb{E}\{A(\mathbf{q})\} &= m_2^2 (\|\mathbf{q}\|^2 \mathbf{I} + \mathbf{q} \mathbf{q}^H) + \kappa \text{ddiag}(\mathbf{q} \mathbf{q}^H), \\ \mathbb{E}\{B(\mathbf{q})\} &= 2m_2^2 \mathbf{q} \mathbf{q}^T + \kappa \text{ddiag}(\mathbf{q} \mathbf{q}^T). \end{aligned}$$

The solutions of the CMA problem of Eq.(5) are of the form $\mathbf{z} = e^{i\theta} \mathbf{e}_{\ell_j}$, with $\ell_j \in \{1, \dots, L\}, \theta \in [0, 2\pi]$. Hence, $\|\mathbf{z}\| = 1$ and the eigenvalues of the matrix $\text{ddiag}(\mathbf{z} \mathbf{z}^H)$ are equal to 1 (with multiplicity 1) and 0 (with multiplicity $L-1$).

Two corollaries are helpful to prove Lemmas 2 and 3:

Corollary 11. *Suppose $K \geq C_1(\delta)L$. Then, with probability at least $1 - 6e^{-c_1(\delta)K}$, for all $\mathbf{h} \in \mathbb{C}^L$ such that $\|\mathbf{h}\| = 1$, we have*

$$(2m_2^2 + \delta) \|\mathbf{h}\|^2 \geq \frac{1}{K} \sum_{k=1}^K |\mathbf{s}_k^H \mathbf{z}|^2 |\mathbf{s}_k^H \mathbf{h}|^2 \geq (m_2^2 + \kappa - \delta) \|\mathbf{h}\|^2.$$

Proof. Note that $\frac{1}{K} \sum_{k=1}^K |\mathbf{s}_k^H \mathbf{z}|^2 |\mathbf{s}_k^H \mathbf{h}|^2 = \mathbf{h}^H A(\mathbf{z}) \mathbf{h}$ and from Lemma 1 it follows that $-\delta \mathbf{I} \preceq A(\mathbf{z}) - \mathbb{E}\{A(\mathbf{z})\} \preceq \delta \mathbf{I}$. With $\kappa < 0$, we obtain

$$\begin{aligned} A(\mathbf{z}) &\succeq m_2^2 (\mathbf{I} + \mathbf{z} \mathbf{z}^H) + \kappa \mathbf{I} - \delta \mathbf{I}, \\ A(\mathbf{z}) &\preceq m_2^2 (\mathbf{I} + \mathbf{z} \mathbf{z}^H) + \delta \mathbf{I}. \quad \blacksquare \end{aligned}$$

Corollary 12. *Suppose $K \geq C_1(\delta)L$. Then, with probability at least $1 - 6e^{-c_1(\delta)K}$, for all $\mathbf{h} \in \mathbb{C}^L$ such that $\|\mathbf{h}\| = 1$, we have*

$$\begin{aligned} &\frac{m_2^2 + \kappa - \delta}{2} \|\mathbf{h}\|^2 + \frac{3}{2} \text{Re}(\mathbf{z}^H \mathbf{h})^2 - \frac{1}{2} \text{Im}(\mathbf{z}^H \mathbf{h})^2 \\ &\leq \frac{1}{K} \sum_{k=1}^K \text{Re}(\mathbf{h}^H \mathbf{s}_k \mathbf{s}_k^H \mathbf{z})^2 \\ &\leq \frac{m_2^2 + \delta}{2} \|\mathbf{h}\|^2 + \frac{3}{2} \text{Re}(\mathbf{z}^H \mathbf{h})^2 - \frac{1}{2} \text{Im}(\mathbf{z}^H \mathbf{h})^2. \end{aligned}$$

Proof. Lemma 1 states that $\delta \mathbf{I} \preceq U(\mathbf{z}) - \mathbb{E}\{U(\mathbf{z})\} \preceq \delta \mathbf{I}$. For the lower bound, recall that $2\text{Re}(c)^2 = |c|^2 + \text{Re}(c^2)$ for $c \in \mathbb{C}$, and

$$\begin{aligned} \frac{1}{K} \sum_{k=1}^K \text{Re}(\mathbf{h}^H \mathbf{s}_k \mathbf{s}_k^H \mathbf{z})^2 &= \frac{1}{4} \begin{bmatrix} \mathbf{h} \\ \bar{\mathbf{h}} \end{bmatrix}^H \begin{bmatrix} A(\mathbf{z}) & B(\mathbf{z}) \\ B(\mathbf{z}) & A(\mathbf{z}) \end{bmatrix} \begin{bmatrix} \mathbf{h} \\ \bar{\mathbf{h}} \end{bmatrix} \\ &\geq \frac{m_2^2 - \delta}{2} \|\mathbf{h}\|^2 + \frac{3}{2} m_2^2 \text{Re}(\mathbf{z}^H \mathbf{h})^2 - \frac{1}{2} m_2^2 \text{Im}(\mathbf{z}^H \mathbf{h})^2 \\ &\quad + \frac{\kappa}{2} \text{Re}(\mathbf{h}^H \text{ddiag}(\mathbf{z} \mathbf{z}^H) \mathbf{h} + \mathbf{h}^H \text{ddiag}(\mathbf{z} \mathbf{z}^T) \bar{\mathbf{h}}). \end{aligned}$$

Note that $\kappa < 0$ and the last factor can be bounded as

$$\begin{aligned} &\frac{\kappa}{2} \text{Re}(\mathbf{h}^H \text{ddiag}(\mathbf{z} \mathbf{z}^H) \mathbf{h} + \mathbf{h}^H \text{ddiag}(\mathbf{z} \mathbf{z}^T) \bar{\mathbf{h}}) \\ &\geq \kappa \sum_{a=1}^L |\bar{z}_a h_a|^2 \geq \kappa \|\mathbf{h}\|^2. \end{aligned}$$

The upper bound is obtained similarly. ■

APPENDIX B: PROOF OF LEMMA 1

Rewrite the Hessian as

$$\begin{aligned} \nabla^2 f(\mathbf{z}) &= \begin{bmatrix} A(\mathbf{z}) & B(\mathbf{z}) \\ B(\mathbf{z}) & A(\mathbf{z}) \end{bmatrix} + \begin{bmatrix} A(\mathbf{z}) & \mathbf{0} \\ \mathbf{0} & A(\mathbf{z}) \end{bmatrix} - R_2 \begin{bmatrix} \mathbf{S} & \mathbf{0} \\ \mathbf{0} & \bar{\mathbf{S}} \end{bmatrix} \\ &= U(\mathbf{z}) + A'(\mathbf{z}) - R_2 \mathbf{S}'. \end{aligned}$$

Observe that $\mathbf{U}(\mathbf{z})$ corresponds to the Hessian of the Phase Retrieval problem, which differs from the CMA Hessian due to the use of a desired average magnitude instead of known sampled amplitudes. Using the triangle inequality, to prove the lemma we show that

$$\|\mathbf{S} - \mathbb{E}\{\mathbf{S}\}\| \leq \delta_S = \delta/(8R_2), \quad (60)$$

$$\|\mathbf{A}(\mathbf{z}) - \mathbb{E}\{\mathbf{A}(\mathbf{z})\}\| \leq \delta_A = \delta/8, \quad (61)$$

$$\|\mathbf{U}(\mathbf{z}) - \mathbb{E}\{\mathbf{U}(\mathbf{z})\}\| \leq \delta_U = \delta/2. \quad (62)$$

Recall that the signal vectors are independent for $k \in \{1, \dots, K\}$. Moreover, QAM constellations are bounded, thus the signal vectors are subgaussian. Hence, via Lemma 9, Eq.(60) holds with probability at least $1 - 2e^{-c_3(\delta_S)K}$ by choosing $K \geq C_3(\delta_S)L$.

Let $\mathbf{a}_k = (\mathbf{s}_k^H \mathbf{z}) \mathbf{s}_k$, which are independent for $k \in \{1, \dots, K\}$. Note that $\mathbf{s}_k^H \mathbf{z} = \sqrt{m_2} e^{i\varphi} s_{\ell_j}[k]$, and therefore the vectors \mathbf{a}_k have bounded, discrete elements over an exponentially large set, and as such they are subgaussian [47]. Additionally, we have

$$\mathbf{A}(\mathbf{z}) = \frac{1}{K} \sum_{k=1}^K \mathbf{a}_k \mathbf{a}_k^H.$$

Therefore, by invoking Lemma 9, Eq.(61) holds with probability at least $1 - 2e^{-c_4(\delta_A)K}$ whenever $K \geq C_4(\delta_A)L$.

Now define $\mathbf{u}_k^H = [\mathbf{a}_k^H \ \mathbf{a}_k^T]$. Using a similar reasoning as above, \mathbf{u}_k are also subgaussian and independent for $k \in \{1, \dots, K\}$, and

$$\mathbf{U}(\mathbf{z}) = \frac{1}{K} \sum_{k=1}^K \mathbf{u}_k \mathbf{u}_k^H.$$

Lemma 9 then states that Eq.(62) holds with probability at least $1 - 2e^{-c_5(\delta/2)K}$ by choosing $K \geq C_5(\delta_U)L$.

Finally, set $C_1(\delta) \geq \max\{C_3(\delta_S), C_4(\delta_A), C_5(\delta_U)\}$. By selecting $K \geq C_1(\delta)L$, Lemma 1 holds with probability at least $1 - 6e^{-c_1(\delta)K}$, where we define $c_1(\delta) = \min\{c_3(\delta_S), c_4(\delta_A), c_5(\delta_U)\}$.

APPENDIX C: PROOF OF LEMMA 2

Let $\mathbf{q} \in E(\epsilon)$ and $\mathbf{h} = e^{-i\phi(\mathbf{q})} \mathbf{q} - \mathbf{z}$. Hence $\|\mathbf{h}\| \leq \epsilon$ and $\text{Im}(\mathbf{h}^H \mathbf{z}) = 0$, as \mathbf{h} and \mathbf{z} are geometrically aligned:

$$\mathbf{h}^H \mathbf{z} = e^{-i\angle(\mathbf{q}^H \mathbf{z})} \mathbf{q}^H \mathbf{z} - \mathbf{z}^H \mathbf{z} = |\mathbf{q}^H \mathbf{z}| - \|\mathbf{z}\|^2 \in \mathbb{R}. \quad (63)$$

Recall that $\nabla f(e^{i\theta} \mathbf{z}) = 0$ for any $\theta \in [0, 2\pi]$, thus the proof is equivalent to proving

$$\begin{aligned} & \text{Re}(\langle \nabla f(\mathbf{q}) - \nabla f(e^{i\phi(\mathbf{q})} \mathbf{z}), \mathbf{q} - e^{i\phi(\mathbf{q})} \mathbf{z} \rangle) \\ &= \frac{1}{K} \sum_{k=1}^K \left(2\text{Re}(\mathbf{h}^H \mathbf{s}_k \mathbf{s}_k^H \mathbf{z})^2 + 3\text{Re}(\mathbf{h}^H \mathbf{s}_k \mathbf{s}_k^H \mathbf{z}) |\mathbf{s}_k^H \mathbf{h}|^2 \right. \\ & \quad \left. + \frac{9}{10} |\mathbf{s}_k^H \mathbf{h}|^4 + (|\mathbf{s}_k^H \mathbf{z}|^2 - R_2) |\mathbf{s}_k^H \mathbf{h}|^2 \right) \\ & \geq \left(\frac{1}{\alpha} + \frac{2m_2^2 - R_2 m_2 + \delta}{4} \right) \|\mathbf{h}\|^2 \end{aligned}$$

for all \mathbf{h} satisfying $\text{Im}(\mathbf{h}^H \mathbf{z}) = 0$ and $\|\mathbf{h}\| \leq \epsilon$. It suffices to show that for all \mathbf{h} such that $\text{Im}(\mathbf{h}^H \mathbf{z}) = 0$ and $\|\mathbf{h}\| = 1$, and for all ξ with $0 \leq \xi \leq \epsilon$, the following inequality holds

$$\begin{aligned} & \frac{1}{K} \sum_{k=1}^K \left(2\text{Re}(\mathbf{h}^H \mathbf{s}_k \mathbf{s}_k^H \mathbf{z})^2 + 3\xi \text{Re}(\mathbf{h}^H \mathbf{s}_k \mathbf{s}_k^H \mathbf{z}) |\mathbf{s}_k^H \mathbf{h}|^2 \right. \\ & \quad \left. + \frac{9}{10} \xi^2 |\mathbf{s}_k^H \mathbf{h}|^4 + (|\mathbf{s}_k^H \mathbf{z}|^2 - R_2) |\mathbf{s}_k^H \mathbf{h}|^2 \right) \\ & \geq \frac{1}{\alpha} + \frac{2m_2^2 - R_2 m_2 + \delta}{4}. \end{aligned}$$

Invoking Corollary 12, we show that for all \mathbf{h} such that $\text{Im}(\mathbf{h}^H \mathbf{z}) = 0$ and $\|\mathbf{h}\| = 1$, and for all ξ with $0 \leq \xi \leq \epsilon$,

$$\begin{aligned} & \frac{1}{K} \sum_{k=1}^K \left(\frac{5}{2} \text{Re}(\mathbf{h}^H \mathbf{s}_k \mathbf{s}_k^H \mathbf{z})^2 + 3\xi \text{Re}(\mathbf{h}^H \mathbf{s}_k \mathbf{s}_k^H \mathbf{z}) |\mathbf{s}_k^H \mathbf{h}|^2 \right. \\ & \quad \left. + \frac{9}{10} \xi^2 |\mathbf{s}_k^H \mathbf{h}|^4 + (|\mathbf{s}_k^H \mathbf{z}|^2 - R_2) |\mathbf{s}_k^H \mathbf{h}|^2 \right) \\ & \geq \frac{1}{\alpha} + \frac{2m_2^2 - R_2 m_2 + \kappa}{2} + \frac{3m_2^2}{4} \text{Re}(\mathbf{z}^H \mathbf{h})^2. \quad (64) \end{aligned}$$

For constant modulus signals, the last averaging term of the LHS of Eq.(64) is zero. For non-constant modulus QAM signals, the term is bounded by Corollaries 10 and 11:

$$\begin{aligned} & \frac{1}{K} \sum_{k=1}^K \left(|\mathbf{s}_k^H \mathbf{h}|^2 |\mathbf{s}_k^H \mathbf{z}|^2 - R_2 |\mathbf{s}_k^H \mathbf{h}|^2 \right) \\ & \geq (m_2^2 - R_2 m_2 + \kappa - (1 + R_2)\delta) \cdot \mathbf{1}[Q \neq 4]. \end{aligned}$$

Let

$$\begin{aligned} \mathbf{Y}(\mathbf{h}, \xi) &= \frac{1}{K} \sum_{k=1}^K \left(\frac{5}{2} \text{Re}(\mathbf{h}^H \mathbf{s}_k \mathbf{s}_k^H \mathbf{z})^2 \right. \\ & \quad \left. + 3\xi \text{Re}(\mathbf{h}^H \mathbf{s}_k \mathbf{s}_k^H \mathbf{z}) |\mathbf{s}_k^H \mathbf{h}|^2 + \frac{9\xi^2}{10} |\mathbf{s}_k^H \mathbf{h}|^4 \right). \end{aligned}$$

Since $(a - b)^2 \geq \frac{a^2}{2} - b^2$, Cauchy-Schwarz inequality leads to

$$\begin{aligned} & \mathbf{Y}(\mathbf{h}, \xi) \\ & \geq \left(\sqrt{\frac{5}{2K} \sum_{k=1}^K \text{Re}(\mathbf{h}^H \mathbf{s}_k \mathbf{s}_k^H \mathbf{z})^2} - \sqrt{\frac{9\xi^2}{10K} \sum_{k=1}^K |\mathbf{s}_k^H \mathbf{h}|^4} \right)^2 \\ & \geq \frac{5}{4K} \sum_{k=1}^K \text{Re}(\mathbf{h}^H \mathbf{s}_k \mathbf{s}_k^H \mathbf{z})^2 - \frac{9\xi^2}{10K} \sum_{k=1}^K |\mathbf{s}_k^H \mathbf{h}|^4. \end{aligned}$$

By means of Corollary 10, with high probability we have

$$\frac{1}{K} \sum_{k=1}^K |\mathbf{s}_k^H \mathbf{h}|^4 \leq \max_k \|\mathbf{s}_k\|^2 \left(\frac{1}{K} \sum_{k=1}^K |\mathbf{s}_k^H \mathbf{h}|^2 \right) \leq B^2 L (m_2 + \delta).$$

Using this result and Corollary 12, if $\|\mathbf{h}\| = 1$, it holds with high probability that

$$\begin{aligned} \mathbf{Y}(\mathbf{h}, \xi) & \geq \frac{5m_2^2}{2} \text{Re}(\mathbf{z}^H \mathbf{h})^2 + \frac{5}{8} (2m_2^2 - R_2 m_2 - \delta) \\ & \quad - \frac{9B^2 L}{10} \xi^2 (m_2 + \delta) + \frac{5}{4} \kappa. \end{aligned}$$

Hence, Lemma 2 holds under the following condition:

$$\begin{aligned} & \frac{5m_2^2}{2} \text{Re}(z^H \mathbf{h})^2 + \frac{5}{8}(2m_2^2 - R_2 m_2 - \delta) - \frac{9B^2 L}{10} \xi^2 (m_2 + \delta) \\ & + \frac{5}{4} \kappa + (m_2^2 - R_2 m_2 + \kappa - (1 + R_2) \delta) \cdot \mathbf{1}[Q \neq 4] \\ & \geq \frac{1}{\alpha} + \frac{2m_2^2 - R_2 m_2 + \kappa}{2} + \frac{3m_2^2}{4} \text{Re}(z^H \mathbf{h})^2. \end{aligned} \quad (65)$$

With $\epsilon = (2B\sqrt{L})^{-1}$ and $\delta \leq 0.1$, Eq.(65) holds for $\alpha \geq 30$.

APPENDIX D: PROOF OF LEMMA 3

Let $\mathbf{q} \in E(\epsilon)$ and $\mathbf{h} = e^{-i\phi(\mathbf{q})} \mathbf{q} - \mathbf{z}$. For any $\mathbf{u} \in \mathbb{C}^L$ such that $\|\mathbf{u}\| = 1$, let $\mathbf{v} = e^{-i\phi(\mathbf{q})} \mathbf{u}$. Recall that $f(e^{i\theta} \mathbf{z}) = 0$ for any $\theta \in [0, 2\pi]$. Therefore, it suffices to show that

$$\begin{aligned} & |\mathbf{u}^H \nabla f(\mathbf{q})|^2 = \left| \mathbf{u}^H (\nabla f(\mathbf{q}) - \nabla f(e^{i\phi(\mathbf{q})} \mathbf{z})) \right|^2 \\ & = \left| \frac{1}{K} \sum_{k=1}^K \mathbf{v}^H \mathbf{s}_k \mathbf{s}_k^H \mathbf{z} \left(|\mathbf{s}_k^H \mathbf{h}|^2 + 2\text{Re}(\mathbf{h}^H \mathbf{s}_k \mathbf{s}_k^H \mathbf{z}) \right) \right. \\ & \quad \left. + \left(|\mathbf{s}_k^H \mathbf{h}|^2 + 2\text{Re}(\mathbf{h}^H \mathbf{s}_k \mathbf{s}_k^H \mathbf{z}) + |\mathbf{s}_k^H \mathbf{z}|^2 - R_2 \right) \mathbf{v}^H \mathbf{s}_k \mathbf{s}_k^H \mathbf{h} \right|^2 \\ & \leq \left(\frac{1}{K} \sum_{k=1}^K 2|\mathbf{s}_k^H \mathbf{z}|^2 |\mathbf{s}_k^H \mathbf{v}| |\mathbf{s}_k^H \mathbf{h}| + 3|\mathbf{s}_k^H \mathbf{z}| |\mathbf{s}_k^H \mathbf{v}| |\mathbf{s}_k^H \mathbf{h}|^2 \right. \\ & \quad \left. + |\mathbf{s}_k^H \mathbf{h}|^3 |\mathbf{s}_k^H \mathbf{v}| \right)^2 + \left| \frac{1}{K} \sum_{k=1}^K (|\mathbf{s}_k^H \mathbf{z}|^2 - R_2) \mathbf{v}^H \mathbf{s}_k \mathbf{s}_k^H \mathbf{h} \right|^2 \\ & \leq \beta \left(\frac{2m_2^2 - R_2 m_2 + \delta}{4} \|\mathbf{h}\|^2 + \frac{1}{10K} \sum_{k=1}^K |\mathbf{s}_k^H \mathbf{h}|^4 \right) \end{aligned}$$

holds for all \mathbf{h} and \mathbf{v} such that $\text{Im}(\mathbf{h}^H \mathbf{z}) = 0$, $\|\mathbf{h}\| \leq \epsilon$, and $\|\mathbf{v}\| = 1$. Equivalently, we prove that for all \mathbf{h} and \mathbf{v} such that $\text{Im}(\mathbf{h}^H \mathbf{z}) = 0$, $\|\mathbf{h}\| = \|\mathbf{v}\| = 1$ and for all ξ with $0 \leq \xi \leq \epsilon$, the following inequality holds

$$\begin{aligned} & \left(\frac{1}{K} \sum_{k=1}^K 2|\mathbf{s}_k^H \mathbf{z}|^2 |\mathbf{s}_k^H \mathbf{v}| |\mathbf{s}_k^H \mathbf{h}| + 3\xi |\mathbf{s}_k^H \mathbf{z}| |\mathbf{s}_k^H \mathbf{v}| |\mathbf{s}_k^H \mathbf{h}|^2 \right. \\ & \quad \left. + \xi^2 |\mathbf{s}_k^H \mathbf{h}|^3 |\mathbf{s}_k^H \mathbf{v}| \right)^2 + \left| \frac{1}{K} \sum_{k=1}^K (|\mathbf{s}_k^H \mathbf{z}|^2 - R_2) \mathbf{v}^H \mathbf{s}_k \mathbf{s}_k^H \mathbf{h} \right|^2 \\ & \leq \beta \left(\frac{2m_2^2 - R_2 m_2 + \delta}{4} + \frac{\xi^2}{10K} \sum_{k=1}^K |\mathbf{s}_k^H \mathbf{h}|^4 \right). \end{aligned}$$

Knowing that $(a + b + c)^2 \leq 3(a^2 + b^2 + c^2)$,

$$\begin{aligned} |\mathbf{u}^H \nabla f(\mathbf{q})|^2 & \leq 12 \left(\frac{1}{K} \sum_{k=1}^K |\mathbf{s}_k^H \mathbf{z}|^2 |\mathbf{s}_k^H \mathbf{v}| |\mathbf{s}_k^H \mathbf{h}| \right)^2 \\ & \quad + 27\xi^2 \left(\frac{1}{K} \sum_{k=1}^K |\mathbf{s}_k^H \mathbf{z}| |\mathbf{s}_k^H \mathbf{v}| |\mathbf{s}_k^H \mathbf{h}|^2 \right)^2 \\ & \quad + 3\xi^4 \left(\frac{1}{K} \sum_{k=1}^K |\mathbf{s}_k^H \mathbf{h}|^3 |\mathbf{s}_k^H \mathbf{v}| \right)^2 \\ & \quad + \left| \frac{1}{K} \sum_{k=1}^K (|\mathbf{s}_k^H \mathbf{z}|^2 - R_2) \mathbf{v}^H \mathbf{s}_k \mathbf{s}_k^H \mathbf{h} \right|^2 \\ & \leq 12I_1 + 27\xi^2 I_2 + 3\xi^4 I_3 + I_4. \end{aligned}$$

We now bound these terms on the right-hand side. By means of the Cauchy-Schwarz inequality and Corollary 11,

$$\begin{aligned} I_1 & \leq \left(\frac{1}{K} \sum_{k=1}^K |\mathbf{s}_k^H \mathbf{z}|^2 |\mathbf{s}_k^H \mathbf{v}|^2 \right) \left(\frac{1}{K} \sum_{k=1}^K |\mathbf{s}_k^H \mathbf{z}|^2 |\mathbf{s}_k^H \mathbf{h}|^2 \right) \\ & \leq (2m_2^2 + \delta)^2, \end{aligned}$$

and

$$\begin{aligned} I_2 & \leq \left(\frac{1}{K} \sum_{k=1}^K |\mathbf{s}_k^H \mathbf{h}|^4 \right) \left(\frac{1}{K} \sum_{k=1}^K |\mathbf{s}_k^H \mathbf{v}|^2 |\mathbf{s}_k^H \mathbf{z}|^2 \right) \\ & \leq \frac{2m_2^2 + \delta}{K} \sum_{k=1}^K |\mathbf{s}_k^H \mathbf{h}|^4. \end{aligned}$$

Invoking Corollary 10, the bounded norm $\|\mathbf{s}_k\| \leq B\sqrt{L}$, and Cauchy-Schwarz inequality, we obtain

$$I_3 \leq \left(\frac{1}{K} \sum_{k=1}^K |\mathbf{s}_k^H \mathbf{h}|^3 \max_k \|\mathbf{s}_k\| \right)^2 \leq \frac{B^2 L (m_2 + \delta)}{K} \sum_{k=1}^K |\mathbf{s}_k^H \mathbf{h}|^4.$$

For constant modulus signals, $I_4 = 0$. For non-constant modulus QAM signals, we can bound this term by invoking the Cauchy-Schwarz inequality:

$$\begin{aligned} I_4 & \leq \left(\frac{1}{K} \sum_{k=1}^K (|\mathbf{s}_k^H \mathbf{z}|^2 - R_2) \right) \left(\frac{1}{K} \sum_{k=1}^K |\mathbf{s}_k^H \mathbf{v}|^2 |\mathbf{s}_k^H \mathbf{h}|^2 \right) \\ & \leq (B^2 - R_2)^2 B^2 L (m_2 + \delta) \|\mathbf{h}\|^2 \cdot \mathbf{1}[Q \neq 4]. \end{aligned}$$

Therefore, we obtain

$$\begin{aligned} \|\nabla f(\mathbf{q})\|^2 & = \max_{\|\mathbf{u}\|=1} \left| \mathbf{u}^H (\nabla f(\mathbf{q}) - \nabla f(e^{i\phi(\mathbf{q})} \mathbf{z})) \right|^2 \\ & \leq 12(2m_2^2 + \delta)^2 \\ & \quad + \frac{27\xi^2 (2m_2^2 + \delta)}{K} \sum_{k=1}^K |\mathbf{s}_k^H \mathbf{h}|^4 \\ & \quad + \frac{3B^2 L \xi^4 (m_2 + \delta)}{K} \sum_{k=1}^K |\mathbf{s}_k^H \mathbf{h}|^4 \\ & \quad + (B^2 - R_2)^2 B^2 L (m_2 + \delta) \cdot \mathbf{1}[Q \neq 4] \\ & \leq \beta \left(\frac{2m_2^2 - R_2 m_2 + \delta}{4} + \frac{\xi^2}{10K} \sum_{k=1}^K |\mathbf{s}_k^H \mathbf{h}|^4 \right). \end{aligned}$$

Hence, Lemma 3 holds under the following condition:

$$\begin{aligned} \beta & \geq \max \left\{ \frac{48(2m_2^2 + \delta)^2}{2m_2^2 - R_2 m_2 + \delta} \right. \\ & \quad \left. + \frac{4(B^2 - R_2)^2 B^2 L (m_2 + \delta)}{2m_2^2 - R_2 m_2 + \delta} \cdot \mathbf{1}[Q \neq 4], \right. \\ & \quad \left. 270(2m_2^2 + \delta) + 30B^2 L \epsilon^2 (m_2 + \delta) \right\}. \end{aligned} \quad (66)$$

With $\epsilon = (2B\sqrt{L})^{-1}$ and $\delta \leq 0.1$, Eq.(66) holds for $\beta \geq 580$.